Diverging trends in aerosol sulfate and nitrate measured in the remote North Atlantic on Barbados are attributed to clean air policies, African smoke, and anthropogenic emissions

Cassandra J. Gaston[1]*; Joseph M. Prospero[1]; Kristen Foley[2]; Havala O.T. Pye[2]; Lillian Custals[1]; Edmund Blades[1]; Peter Sealy[1]; James A. Christie[1]

[1]Rosenstiel School of Marine, Atmospheric, and Earth Science, University of Miami, Miami, FL 33149, USA

[2]Office of Research and Development, U.S. Environmental Protection Agency, Research Triangle Park, North Carolina, USA

*Correspondence to: cgaston@miami.edu; Ph: 305-421-4979

**ABSTRACT**

Sulfate and nitrate aerosols degrade air quality, modulate radiative forcing and the hydrological cycle, and affect biogeochemical cycles, yet their global cycles are poorly understood. Here, we examined trends in 21 years of aerosol measurements made at Ragged Point, Barbados, the easternmost promontory on the island located in the eastern Caribbean Basin. Though the site has historically been used to characterize African dust transport, here we focused on changes in nitrate and non-sea salt (nss) sulfate aerosol from 1990-2011. Nitrate aerosol concentrations averaged over the entire period were stable at 0.59 $\mu g/m^3$ ± 0.04 $\mu g/m^3$ except for elevated nitrate concentrations in the spring of 2010 as well as during the summer and fall of 2008 due to the transport of biomass burning emissions from both northern and southern Africa to our site. In contrast, from 1990 to 2000, nss-sulfate decreased 30% at a rate of 0.023 $\mu g/m^3/yr$, a trend which we attribute to air quality policies enacted in the U.S. and Europe. From 2000-2011, sulfate gradually increased at a rate of 0.021 $\mu g/m^3/yr$ to pre-1990s levels of 0.90 $\mu g/m^3$. We used the Community Multiscale Air Quality (CMAQ) model simulations from the EPA's Air QUAlity TimE Series (EQUATES) to better understand the changes in nss-sulfate after 2000. The model simulations estimate that increases in anthropogenic emissions from Africa explain the increase in nss-sulfate observed in Barbados. Our results highlight the need to better constrain emissions from developing countries and to assess their impact on aerosol burdens in remote source regions.

## 1. INTRODUCTION

Sulfate and nitrate aerosol, formed from gaseous sulfur dioxide ($SO_2$) and nitrogen oxides (e.g., $NO_x \equiv NO+NO_2$) as well as reactive nitrogen (e.g., $NO_y$), contribute to aerosol direct and indirect radiative forcing, impact biogeochemical cycles (Jickells et al., 2017), and degrade air quality (Adams et al., 1999; Appel et al., 1978; Charlson et al., 1992; Lelieveld & Heintzenberg, 1992; Murphy et al., 2006). An outstanding question is, how have sulfate and nitrate aerosol burdens in remote regions changed in response to air quality policies, economic growth, and changing frequency of wildfires—all of which have affected $SO_2$ and $NO_x$ emissions? Answering this question is important as remote regions are an important barometer of changing global emission inventories, contain ecosystems sensitive to changing chemical inputs (Galloway et al., 2008; Mahowald et al., 2017), and are most sensitive to fluctuations in aerosol burdens that alter aerosol-cloud interactions (Carslaw et al., 2013). Long-term measurement records in remote regions can provide insight into this question as well as further advance current chemical transport and global climate models. However, there are few long-term measurement records in remote regions. In this work, we leverage 21 years of nitrate and sulfate aerosol concentrations measured at Ragged Point, Barbados, a remote site in the eastern North Atlantic marine boundary layer, and use simulations from a hemispheric chemical transport model—the Community Multiscale Air Quality (CMAQ) model within the EPA's Air QUAlity TimE Series (EQUATES) (Foley et al., 2023)—to link our observed changes in nitrate and sulfate to changing emissions inventories and meteorological conditions. In turn, comparing the EQUATES model output to our time series provides guidance on where in-situ measurements are needed to improve emissions inventories and measurement-model agreement.

Ragged Point, Barbados provides a unique opportunity to understand changes in the nitrate and sulfate aerosol burden in the remote North Atlantic marine boundary layer. Aerosol sampling began in 1971 and continues to this day generating an~50-year measurement record—the longest modern speciated aerosol record, to the best of our knowledge (Prospero et al., 2021; Prospero & Mayol-Bracero, 2013). The site serves as a lynchpin for understanding the impact of long-range aerosol transport on the remote North Atlantic marine boundary layer and Caribbean. The site's primary objective has been to understand the factors affecting the long-range transport of African dust to the Caribbean and North America, which peaks in boreal summer in association with the seasonal northward shift in the intertropical convergence zone (ITCZ). Summer dust events are caused by the strong heating of northern Africa, which causes hot, dry dust-laden desert air to be carried to high altitudes, e.g., 4 – 6 km. African Easterly Waves propagate dust westward within an elevated air layer known as the Saharan Air Layer (SAL) that overrides the cool, moist marine boundary layer (Adams et al., 2012; Carlson & Prospero, 1972; Goudie & Middleton, 2001; Tsamalis et al., 2013). Background emissions at the site are dominated by sea spray and marine biogenic emissions of dimethyl sulfide (DMS) that contribute non-sea salt (nss)-sulfate (Andreae et al., 1985; Barnes et al., 2006; Savoie et al., 2002). Along with dust, anthropogenic emissions from Europe (Lelieveld et al., 2002), North America, and northern Africa are also transported to Barbados (Savoie et al., 2002). Transport from Africa takes ~5-7 days to reach our site while transport from the U.S. and Europe takes longer, typically 7-10 days.

Anthropogenic emissions of $SO_2$ and $NO_x$ that impact Ragged Point have changed in recent decades due to the opposing effects of decreasing emissions mandated by national air quality policies, implemented mostly in developed countries, and increasing emissions linked to rapid economic growth in developing countries. The United States (U.S.) curbed emissions of $NO_x$ and $SO_2$ with the implementation of the Clean Air Act (amended in 1990), resulting in a 92% reduction in $SO_2$ and a 71% reduction in $NO_x$ emissions from 1990-2022 (Aas et al., 2019; Hand et al., 2012; *https://gispub.epa.gov/air/trendsreport/2023/*; Smith et al., 2011; Zhao et al., 2017). Countries within the European Union (EU) passed similar policies resulting in analogous reductions (Aas et al., 2019; Rafaj et al., 2015; Smith et al., 2011; Yang et al., 2020). Notably, reductions in $SO_2$ can reduce aerosol acidity resulting in increased nitrate aerosol. Further, reductions in pollutant gases can relieve oxidant limitations leading to more efficient oxidation and, therefore, reductions in $SO_2$ and $NO_x$ may not reduce sulfate and nitrate aerosol as much as expected (Shah et al., 2018). In contrast to the U.S. and EU, emissions in regions such as the Middle East, India, and Africa are continuing to increase due to rapid economic growth with emissions from India predicted to overtake China as the world's largest emitter of $SO_2$ (Lelieveld et al., 2009; Li et al., 2017; McDuffie et al., 2020). Due to a lack of in-situ measurements in many of these regions, chemical transport and emissions inventory models combined with remote sensing have been key tools to understand changing pollutants.

In addition to fossil fuel emissions, biomass burning is also a major source of $SO_2$ and $NO_x$ that can impact the Atlantic (Andreae, 2019; Andreae & Merlet, 2001; Rickly et al., 2022; Roberts et al., 2009; Zuidema et al., 2018). Wildfire activity has a distinct seasonality linked to the dry seasons in Africa. Burning is most intense in Sub-Saharan Africa from the equator to 20ºN from November through May while from May through October, the savannah regions of Sub-Saharan Africa from the equator to 25ºS are the most active fire sources (Giglio et al., 2006; Kganyago & Shikwambana, 2019; Roberts et al., 2009; Van der Werf et al., 2003). African smoke can be transported to Barbados from Sub-Saharan Africa north of the equator in winter and spring (Quinn et al., 2022; Royer et al., 2023; Wex et al., 2016) and, less frequently, from southern hemispheric Africa in fall (Trapp et al., 2010). Conditions thought to be related to African climate (e.g., the North Atlantic Oscillation and the position of the Azores High) can cause large quantities of northern African dust (and smoke) to be transported during the winter and spring in elevated, mixed aerosol layers (Chiapello et al., 2005; Doherty et al., 2008, 2012; Gutleben et al., 2022) when dust is also carried to northeastern South America (Barkley et al., 2019; Prospero et al., 1981, 2014). Prescribed burns in the southeastern U.S. in winter and spring may also contribute biomass burning emissions to the aerosol burden observed in Barbados (Nowell et al., 2018).

Here we highlight different trends in nitrate and sulfate aerosol over the remote North Atlantic marine boundary layer and relate them to changing emissions. We then compare our observations to simulated concentrations of nitrate and sulfate aerosol using the CMAQ model from EQUATES, which was chosen due to its skill at modeling changes in nitrate and sulfate chemistry within the U.S. (Benish et al., 2022) as well as its ability to simulate constituents and sources of air pollution in remote regions, such as Dhaka, Bangladesh (Sarwar et al., 2023). Our results highlight the importance of long-term atmospheric observations to understand the net outcome of changing

113 global $SO_2$ and $NO_x$ emissions on both the aerosol burden as well as air quality in distant
114 populations.

115

## 2. METHODS

117 **2.1 Aerosol Collection at the Barbados Atmospheric Chemistry Observatory:** Aerosols were
118 collected daily at the University of Miami's Barbados Atmospheric Chemistry Observatory (UM
119 BACO: https://baco.rsmas.miami.edu/) located at Ragged Point, Barbados—the easternmost
120 promontory on the east coast of the island (13.16504N, 59.43207W). The site has been operated
121 by UM since 1971, and aerosol data has been used to document the long-range transport of African
122 dust to the Caribbean and the Americas carried by the easterly trade winds as it is the first landmass
123 encountered by African emissions transported across the Atlantic Ocean (Prospero et al., 2021).
124 The site is approximately 4500 km from the west coast of northern Africa, 3000 km from the east
125 coast of the U.S. and 6000 km from the west coast of the EU. Since 1989, aerosols have been
126 collected at the top of a 17-m sampling tower that stands atop a 30-m bluff (see Fig 1).



127

128 **Figure 1:** Photo of the Barbados Atmospheric Chemistry Observatory (BACO) including the 17-
129 m sampling tower, two shipping container laboratories, and an Advanced Global Atmospheric
130 Gases Experiment (AGAGE) laboratory.

131 A high-volume sampler pulls air at a nominal rate of 0.75 $m^3$/minute across a 20cm x 25cm
132 Whatman-41 filter. The upper particle size limit for our filter collection method is approximately
133 80-100µm or greater based on the geometry of our sampling rain hat (Barkley et al., 2021). Filters
134 were collected daily (e.g., every 24 hours); however, a few multiday samples were also collected

5

that typically span 2 days. Mass collection efficiencies are 90% for sulfate, 95% for nitrate, and 99% for dust (Savoie & Prospero, 1982). Filters are then folded into quarters under a laminar flow hood, placed in a clean Ziploc bag, and periodically shipped to UM for processing. To ensure that local island emissions are not sampled, the sampling pump is only operational when the wind blows directly from the ocean (from 335 degrees through N and E to 130 degrees) with speeds greater than 1 m/s. A timer is used to record the "run time", the total amount of time that the sampling pumps are on during the sampling interval between filter changes. Data with a run time less than 10% of the sampling interval are discarded to minimize the impact of low-speed and flukey wind conditions that might carry aerosols from local sources. These deletions account for less than 10% of all data collected over the record highlighting the steady easterly winds measured at the site year-round. Procedural blanks are collected weekly by placing a Whatman-41 filter in the filter cassette with the sampling pump off for 15 minutes then placing the filter in a clean Ziploc bag; the blank is subsequently processed along with the daily filter samples.

This work focuses on aerosol measurements conducted over 1990-2011, a period that overlaps with the implementation of more stringent air quality policies in the U.S. and Europe. Seasonal trends are also shown where winter is represented by December (from the previous year), January, February (DJF); spring is March, April, May (MAM); summer is June, July, August (JJA); fall is September, October, November (SON). African dust peaks annually at BACO in JJA with episodic transport in DJF and MAM in some years (Prospero & Mayol-Bracero, 2013; Quinn et al., 2022; Royer et al., 2023). Trends presented in this work are derived from Theil-Sen regression. Significance is calculated using paired samples t-tests.

**2.2 Quantification of Dust and Soluble Ion Mass Concentrations:** A one-quarter filter section is extracted three times with a total volume of 20 mL of Milli-Q water to remove soluble material. The extracted filter is placed in a combustion oven (500°C) overnight. The resulting ash is weighed ($m_{filter\ ash}$) and subsequently corrected for the blank by subtracting the ash obtained from performing the same technique on the procedural blank ($m_{procedural\ blank}$). The gross ash weight is adjusted by a factor of 1.3 to account for losses during the extraction and combustion process (Prospero, 1999; Zuidema et al., 2019). This corrected ash mass concentration is equated to mineral dust concentrations present on the filter based on previous comparisons between filter ash and concentrations of aluminum, a tracer for mineral dust (Prospero, 1999; Trapp et al., 2010).

$$Dust = (m_{filter\ ash} - m_{procedural\ blank\ ash}) * 1.3 \tag{1}$$

The filtrate from the sample extraction process and procedural blanks are used to quantify soluble ion concentrations. Anions (e.g., chloride ($Cl^-$), nitrate ($NO_3^-$), and sulfate ($SO_4^{2-}$)) were measured using ion chromatography (IC). Cations (sodium ($Na^+$), potassium ($K^+$), and calcium ($Ca^{2+}$)) were measured with a flame photometer after 2004 while flame atomic absorption spectrophotometry was used prior to 2004 limiting cation analysis to sodium (Savoie, et al., 2002). In addition to total soluble ion concentrations, we also report concentrations of non-sea salt (nss) sulfate, which is a useful tracer of sulfur from marine biogenic and pollution emissions, and nss-potassium, a tracer of biomass burning emissions (Andreae, 1983; Keene et al., 1986). Concentrations of nss-$SO_4^{2-}$ and nss-$K^+$ are calculated using the following mass-based equations and assuming that $Na^+$ is a conservative tracer of sea spray aerosol:

6

176 $$nss - SO_4^{2-} = [SO_4^{2-}] - (0.2517 * [Na^+]) \tag{2}$$

177 $$nss - K^+ = [K^+] - (0.03595 * [Na^+]) \tag{3}$$

178 Filter samples with undetectable amounts of dust and soluble ions compared to procedural blanks
179 are removed from our analysis.

## 2.3 EQUATES Model Products

181 EPA's Air QUAlity TimE Series (EQUATES) Project uses the Community Multiscale Air Quality
182 (CMAQ) model, a 3-D chemical transport air quality model, to simulate air quality over a
183 continuous 2002-2019 period (Foley et al., 2023). CMAQ accounts for gas, cloud, and aerosol
184 chemistry, including processes such as in-cloud sulfate formation from the oxidation of $SO_2$.
185 EQUATES uses CMAQv5.3.2 (Appel et al., 2021) to model the Northern Hemisphere using 108-
186 km resolution and 44 vertical layers (Mathur et al., 2017). Meteorological data are derived from
187 the Weather Research and Forecasting model (WRFv.4.1.1). Emissions from outside the
188 contiguous U.S. and China are generated using the Hemispheric Transport of Air Pollution version
189 2 inventory for the year 2010 (HTAPv2.2) and are scaled to other years using the Community
190 Emissions Data System (CEDS) for the years 2002-2019. The Fire INventory from NCAR (FINN)
191 is used to generate biomass burning emissions (Wiedinmyer et al., 2011), lightning NOx emissions
192 are derived from the Global Emissions IniAtive (GEIA), biogenic volatile organic compounds
193 (VOCs) are from MEGAN2, and soil $NO_x$ is from CAMSv2.1.

194 In this study, EQUATES was used to better understand observed trends, namely in nss-sulfate,
195 after 2000 when observed concentrations unexpectedly increased. EQUATES also simulated
196 concentrations of locally emitted gases, including $SO_2(g)$ and $NO_x(g)$, which are not measured at
197 Ragged Point. The model product is not available for the years prior to 2000. The analysis focused
198 on dust, sea spray, nitrate, sulfate, and gaseous $SO_2$ and $NO_2$. In addition to anthropogenic sources
199 of $SO_2$, natural sources from the oxidation of DMS were included in model runs. Species
200 predictions were extracted from the lowest CMAQ model layer (~10m in thickness) for a source
201 area over the Atlantic Ocean to the east of the island from 59.5627°W to 56.5448°W longitude and
202 14.3989°N to 11.4566°N latitude (equivalent to 16 grid cells with one cell over Ragged Point and
203 the others to the east of the site). Simulated concentrations of aerosol sulfate, nitrate, calcium,
204 potassium, and sodium were obtained for fine mode aerosol (e.g., Aitken and accumulation mode,
205 PMF model outputs) and coarse mode aerosol (Total PM – PM$_{2.5}$, PMC model outputs). Previous
206 studies have shown that most of the aerosol mass at Ragged Point is below 10 μm diameter
207 (Prospero et al., 2001). Because aerosol filters collected at BACO capture total suspended
208 particulate matter, model outputs of fine and coarse mode aerosol concentrations were combined
209 (e.g., PMF + PMC model outputs) to give total aerosol mass concentrations of sulfate, nitrate,
210 sodium, potassium, and calcium. Total concentrations of nss-sulfate and nss-potassium were
211 calculated using Equations 2 and 3, respectively, and model outputs of total sodium mass
212 concentrations, total sulfate mass concentrations, and total potassium mass concentrations from
213 combined coarse and fine mode aerosol model outputs. We calculated concentrations of nss-
214 calcium, which has been shown to be a good tracer for mineral dust in Barbados (Savoie &
215 Prospero, 1980), and dust mass concentrations were then calculated using the average upper crustal

7

216　abundance of calcium in soil (an average of 4.1%) (Scheuvens et al., 2013; Taylor & McLennan,
217　1985) as shown in Equations 4 and 5.

218　$nss - Ca^{2+} = [Ca^{2+}] - (0.0376 * [Na^+])$ （4）

219　$Dust = [nss - Ca^{2+}] * 24.1$ （5）

220　We first assessed the ability of the EQUATES CMAQ simulations to capture trends in different
221　aerosol types observed at Ragged Point. Simulations of sodium and dust from EQUATES capture
222　seasonal and monthly observed trends in dust (see Fig S1 and S2 of the Supporting Information
223　(SI)). However, the model overpredicts sodium (Na$^+$, a proxy for sea spray) by a factor of 3-4 (Fig
224　S1) and underpredicts dust by an average factor of ~7. This low bias for dust in CMAQv5.3.2 is
225　consistent with CMAQ development that occurred after the EQUATES simulations were
226　complete.  A bugfix to the online dust emissions module in CMAQv5.4 increases dust emissions
227　by a factor of 3-7 over the Sahara Desert and parts of Asia (see the CMAQv5.4 release notes for
228　further information; https://www.epa.gov/cmaq/cmaq-documentation#release-notes).

229　In addition to simulating observed aerosol concentrations, EQUATES was also used to examine
230　trends in gaseous indicators of anthropogenic and biomass burning emissions, oxidant
231　concentrations and oxidant ratios important for investigating changes in the oxidation efficiency
232　of locally emitted pollutant gases and the subsequent formation of nitrate and sulfate aerosol.
233　Further, EQUATES was used to investigate whether the oxidation efficiency of SO$_2$(g) changed
234　during the 2002-2011 period. The oxidation ratio was calculated from Equation 6 (Shah et al.,
235　2018):

236　$Oxidation\ Ratio = \dfrac{nss - SO_4^{2-}}{nss - SO_4^{2-} + SO_2}$ （6）

237　For this calculation, we used EQUATES model data for SO$_2$(g) concentrations and filter-based
238　observations of nss-sulfate.

239　**2.4 HYSPLIT Back-trajectory Analysis**

240　Air mass back-trajectory analysis was performed using NOAA's Hybrid Single-Particle
241　Lagrangian Integrated Trajectory (HYSPLIT) model (Draxler & Rolph, 2011; Rolph et al., 2017;
242　Stein et al., 2015). 13-day back-trajectories were initiated at heights of 500, 1000, and 2000-m to
243　capture both SAL and boundary layer transport. Frequency plots were also generated for the entire
244　sampling period (1990-2011) to illustrate seasonal differences in air mass transport and origin and
245　to explore any interannual variability. We used the global National Center for Environmental
246　Prediction (NCEP) reanalysis data that extends back to the beginning of our dataset in 1990
247　(Kramer et al., 2020). The finer resolution Global Data Assimilation System (GDAS) dataset (1°
248　resolution) was used to examine trends in air mass back trajectories in 2008, 2009, and 2010 when
249　transport conditions strongly impacted nitrate aerosol concentrations. We emphasize the
250　challenges in characterizing long-range transported aerosol due to the remoteness of the site, the
251　location of Barbados in the middle of the ocean, and the fact that air layers of smoke and dust
252　change in height during transport. As such, we caution against the over-reliance on HYSPLIT

255 **3. RESULTS**

256 **3.1 Measured Trends from 1990-2011 at Ragged Point.**

257 Figure 2 shows yearly averaged mass concentrations of non-sea salt (nss) sulfate and nitrate
258 from 1990 through 2011. Nitrate concentrations are remarkably stable from 1990 to 2011
259 ($R^2=0.006$, p>0.05 (not significant)) with an average concentration of 0.59 $\mu g/m^3$ ± 0.04 $\mu g/m^3$.
260 However, two anomalous peaks in nitrate are observed in 2008 and 2010 with annual average
261 nitrate concentrations of 0.73 and 0.81 $\mu g/m^3$, respectively. Similarly, dust mass concentrations
262 also show no trend over this period ($R^2=0.06$). In contrast, nss-sulfate decreases by 30% from an
263 average concentration of 0.84 $\mu g/m^3$ starting in 1990 to a minimum of 0.64 $\mu g/m^3$ in 2000 at a rate
264 of -0.023 ug/m³/yr. Subsequently, sulfate gradually increased to 0.91 $\mu g/m^3$ in 2010 and 0.90
265 $\mu g/m^3$ in 2011, maximums across the entire record. The trends in the yearly average mass
266 concentrations of nitrate and nss-sulfate are significantly different (p-value < 0.005), which can be
267 explained by either different sources or different rates of change for precursor $NO_x$ and $SO_2$
268 emissions or different responses in nitrate and sulfate aerosol production to changing emissions of
269 $NO_x$ and $SO_2$ as has been shown in North America (Shah et al., 2018; Vasilakos et al., 2018).
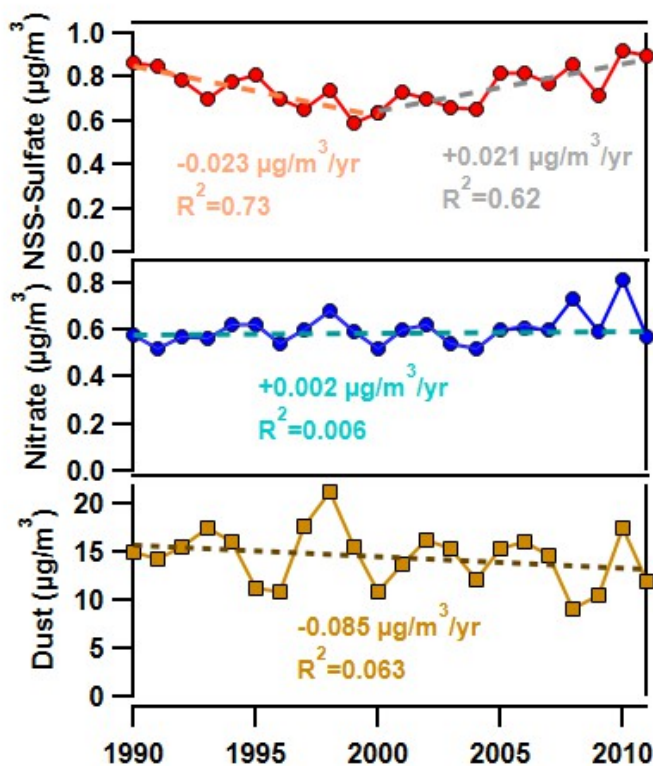


270

271 **Figure 2:** Yearly averages of non-sea salt sulfate (NSS Sulfate, red line, top panel), nitrate (middle panel,
272 blue line), and dust (bottom panel, brown line with squares) measured at Ragged Point, Barbados, from

1990-2011. Dashed lines show changes in NSS Sulfate pre-2000 (orange), post-2000 (gray line), nitrate (teal line) without the spikes in 2008 and 2010 considered, and dust (brown line) over the 1990-2011 period.

The Barbados yearly concentrations differ from long-term observations of aerosol and precipitation chemistry measured at Tudor Hill, a site on the west coast of Bermuda, from 1989-1997 and from 2006-2009 as part of the same program as that at Barbados (AEROCE) and using the same protocols including sampling only when winds are over the ocean (Keene et al., 2014; Savoie, et al., 2002). At the Bermuda site, the prevailing winds come from the West so that the sampling sector extends from 180º through West to 330º. Aerosol nitrate is constant at both sites. However, the nitrate annual mean at Bermuda is ~1.05 $\mu g/m^3$, roughly double the nitrate observed at Ragged Point (Keene et al., 2014; Savoie, et al., 2002). Also, the decline in nss-sulfate observed in Bermuda, from ~2.59 $\mu g/m^3$ in 1989 to ~1.63 $\mu g/m^3$ in 2009, is greater than our observations at Ragged Point (Keene et al., 2014). Furthermore, sulfate aerosol in Bermuda declines over the entire record and does not exhibit the same reversal in the 2000s that we observe at Barbados. The difference in concentrations and trend in nss-sulfate observed at Ragged Point compared to that at Bermuda is not surprising given that the Bermuda site is located 1100 km from the east coast of the U.S. and is more directly influenced by anthropogenic emissions compared to Barbados, which is more remote and could be influenced by a multitude of emission sources (Savoie, et al., 2002). Also, the trend in nss-sulfate at Barbados differs from long-term observations measured at an IMPROVE site in the Virgin Islands. Sulfate shows no trend from 2004-2021 (Hand et al., 2024). The difference in trend in nss-sulfate between Ragged Point and the IMPROVE site in the U.S. Virgin Islands is likely due to more influence from the U.S. and less influence from African emissions. Further, the IMPROVE site does not follow a sector-controlled sampling protocol as does the site in Barbados.

To assess whether annual trends in nss-sulfate and nitrate observed in Barbados are associated with African aerosol transport conditions, annual average measured dust mass concentrations are also shown in Fig 2 and show no appreciable increase or decrease from 1990-2011 ($R^2$=0.06). Therefore, annual trends in nss-sulfate aerosol, which show a decrease from 1990-2000 and an increase from 2000-2011, are not correlated with African dust mass concentrations ($R^2$=0.001). This suggests that the increase in nss-sulfate after the year 2000 is not due to an increase in sulfate associated with heterogeneous reactions between $SO_2(g)$ and dust or to more favorable transport from Africa. Nitrate aerosol, in contrast, is modestly correlated with dust ($R^2$=0.30). Comparing seasonal nitrate and dust mass concentrations by year reveals tighter correlations between nitrate and dust for DJF and MAM (0.46 and 0.4, respectively, see Fig S3). DJF and MAM are not the peak dust transport seasons to the Caribbean, but they are the seasons that favor co-transport of dust and biomass burning emissions from Sub-Saharan Africa north of the equator (Royer et al., 2023). Transport of African smoke to Barbados has been shown to be associated with elevated concentrations of nitrate, which likely explains the association between winter- and spring-time dust and nitrate (Quinn et al., 2021; Savoie & Prospero, 1982).

**3.1.2 Seasonal Patterns in Air Mass Trajectories and Nitrate Concentrations**

HYSPLIT air mass back-trajectories reveal similar seasonal patterns each year with predominantly easterly transport to the site year-round (see Fig S4, which shows 5-day air mass back-trajectory frequency plots for the entire 1990-2011 period and similar patterns year to year). As has been documented in prior work (Prospero et al., 2021), the dominant transport pathways are over the ocean and traversing the African continent. Some trajectories do intercept North America and come close to Europe while few (<10%) air masses come near South America, which is outside of our sampling sector. Air masses typically take 5-7 days to be transported from northern Africa and longer than 7 days to intercept the E.U. and North America. From Figure S4, DJF has some trajectories that intercept North America and some from the northern part of the Atlantic Ocean toward Europe, MAM trajectories are easterly, JJA trajectories are from the west coast of Africa, and SON trajectories are from the east with some from the southeast. We note that the directional tendencies of the trajectories did not noticeably change in 2000, when the concentration trends in nss-sulfate changed.

Figure 3 shows trends in nss-sulfate and nitrate during different seasons (e.g., DJF, MAM, JJA, and SON). Increases in nitrate in 2008 are driven by high nitrate concentrations in JJA and SON in 2008, with most of the increase in September, while high nitrate levels in 2010 are primarily observed during MAM. In 2010, a transition from an El Niño to the strongest La Niña event on record occurred (Wolter & Timlin, 2011; Zhang et al., 2019), and long-range transport from Africa was anomalously high during the springtime as evidenced by high mass concentrations of dust in the spring of 2010 (Zuidema et al., 2019). Daily air mass back-trajectories passed more frequently over the African continent in MAM of 2010 compared to MAM of 2009 (26 vs 6 days) (Fig 4a and b), and nitrate levels exceeded 1 $\mu$g/m$^3$ on over half of those days when trajectories traversed the northern African continent. Figure 4 focuses on trajectories initiated at 500-m height. If trajectories initiated at 1000-m are also included, then transport over the North African continent occurs on 36 days in MAM of 2010, i.e., 82% of days when nitrate levels exceeded 1 $\mu$g/m$^3$. However, during the summertime peak (JJA) in African dust transport in 2010, nitrate does not show the same increase as dust despite frequent transport from northern Africa (see Fig 4d). Further, Fig 4c and 4d compare daily and monthly mean concentrations of nitrate, dust, and non-sea salt potassium (e.g., nss-K$^+$), which is a marker for biomass burning emissions (Andreae & Merlet, 2001). Nitrate and nss-K$^+$ clearly track each other and are both elevated in the spring of 2010. Although biomass burning peaks in December and January while MAM is the tail end of the burn season in northern Sub-Saharan Africa (Giglio et al., 2013; Roberts et al., 2009), the high nitrate loadings observed in 2010 in spring are likely due to strongly favorable transport conditions that transport both dust and smoke to Barbados during this year.
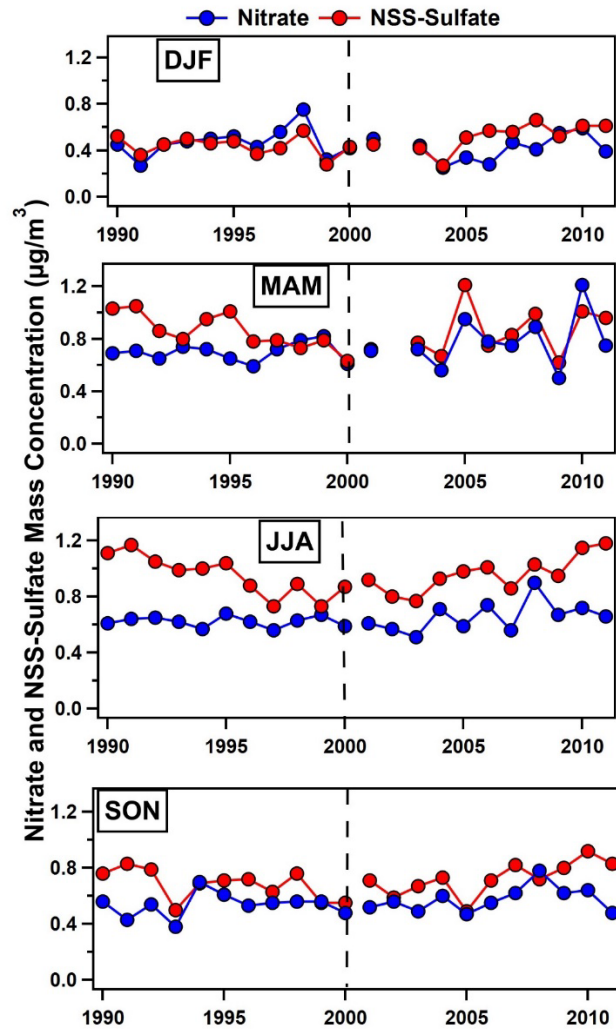
**Figure 3:** Average concentrations of nitrate (blue markers), and nss-sulfate (red markers) for winter (DJF), spring (MAM), summer (JJA), and fall (SON). The vertical black dashed line denotes the year 2000 when nss-sulfate trends shifted from decreasing to increasing.
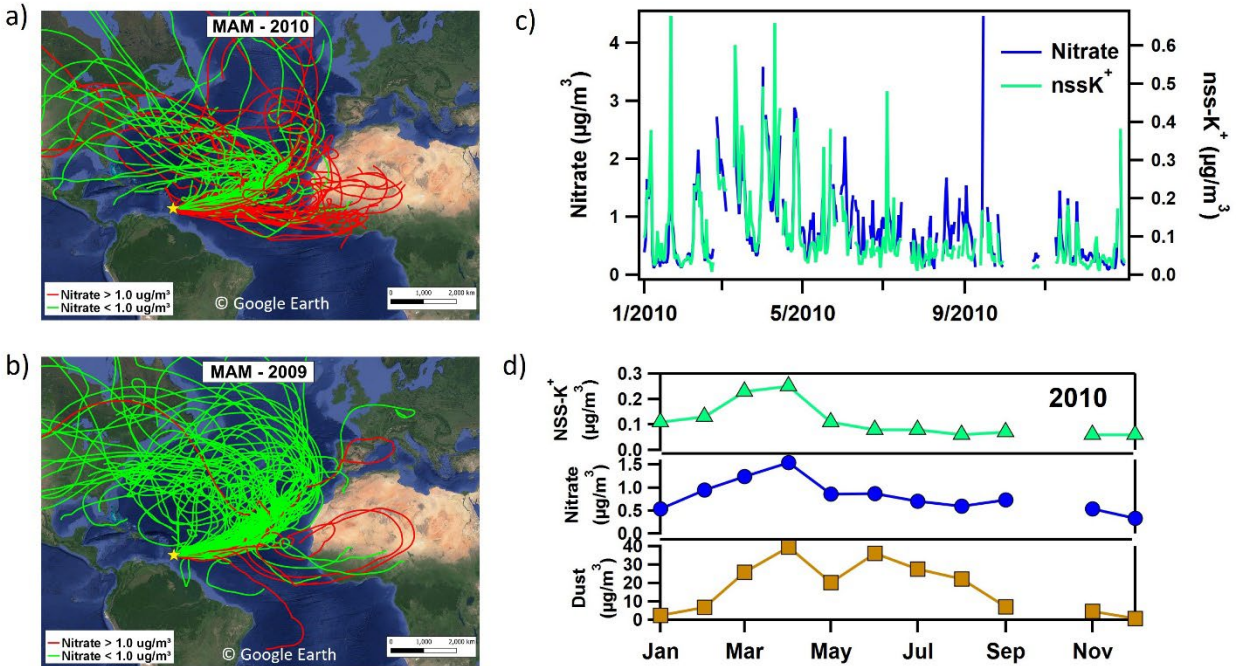
**Figure 4:** 13-day air mass back-trajectories initiated at 500-m for MAM a) 2010 and b) 2009. Back-trajectories labeled in green are for days where nitrate concentrations measured at Ragged Point were < 1 $\mu g/m^3$ while trajectories labeled in red had nitrate > 1 $\mu g/m^3$. Maps are from Google Earth. c) Daily comparison of nitrate and non-sea salt potassium (nss-$K^+$), a biomass burning marker, show a tight correlation ($R^2$=0.62). d) Monthly average concentrations of dust (brown), nitrate (blue), and nss-$K^+$ (green) for 2010.

Similar to 2010, air mass back-trajectories traversed the African continent on just 40% of the days in JJA but 82% of days in September of 2008 with nitrate concentrations > 1 $\mu g/m^3$ (Fig S5 and Fig 5a). If trajectories initiated at the 1000-m level are included, then African transport occurs on 64% of days in JJA with nitrate concentrations > 1 $\mu g/m^3$, consistent with higher level transport in JJA. In JJA, most of the air mass back-trajectories pass through Africa north of the equator. However, in September, trajectories take a more southerly route traversing near the South American coast and Sub-Saharan Africa south of the equator (Fig 5a). Figure 5b shows trajectories for September but in 2009, when fewer trajectories take a southerly route and nitrate concentrations rarely exceed 1 $\mu g/m^3$. September is during the peak of the burn season in Sub-Saharan Africa south of the equator and also dovetails with strong smoke transport over the Atlantic Ocean due to the increased intensity of the African Easterly Jet (Adams et al., 2012; Adebiyi & Zuidema, 2016; Zuidema et al., 2018). Air mass back-trajectories in September from Sub-Saharan Africa south of the equator to our measurement sites in Barbados and Cayenne have been linked with African smoke transport (Barkley et al., 2019; Trapp et al., 2010) further suggesting a link between elevated concentrations of nitrate measured at Barbados with transported African smoke. Biomass burning in the Amazon also peaks in SON (Adams et al., 2012) and could also explain some of the increase in nitrate in this season in 2008.

13
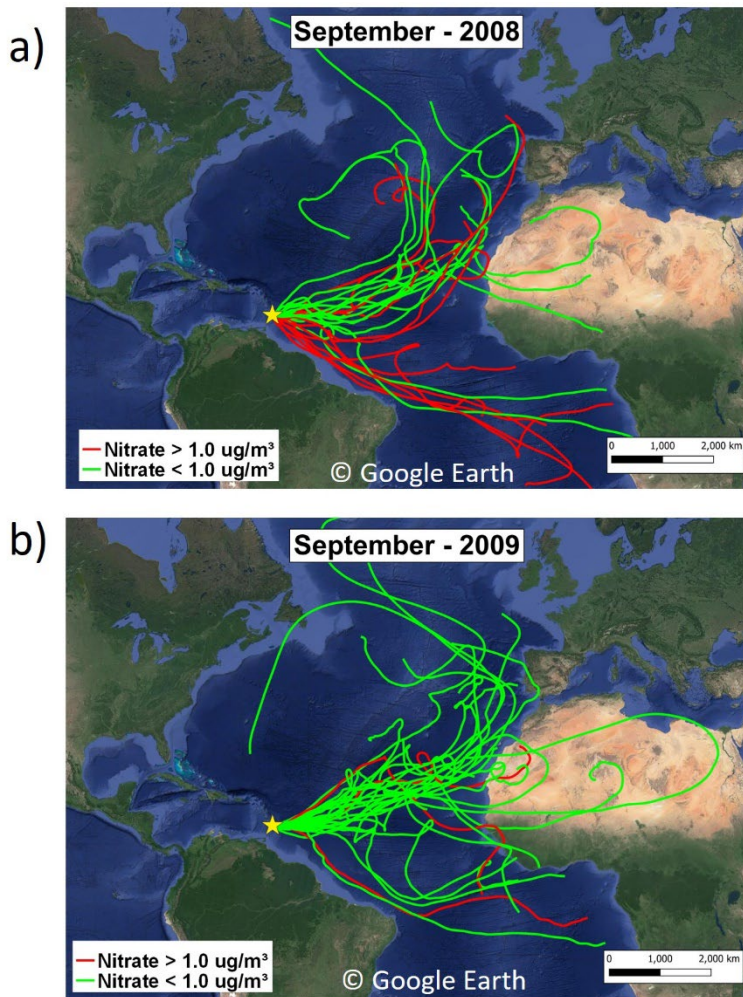
**Figure 5:** 13-day air mass back-trajectories initiated at 500-m for September a) 2008 and b) 2009. Back-trajectories labeled in green are for days when nitrate concentrations measured at Ragged Point were < 1 $\mu$g/m$^3$ while trajectories labeled in red had nitrate > 1 $\mu$g/m$^3$. The maps are from Google Earth.

### 3.1.3 Trends in Non-Sea Salt-Sulfate and Emissions of SO$_2$

Figure 3 reveals that the decrease in sulfate and subsequent increase are measured during most seasons. Table 1 further provides correlation coefficients and the rate of change in either nitrate or sulfate in $\mu$g m$^{-3}$yr$^{-1}$ for data collected pre- and post-2000 when the trend in nss-sulfate changed. Pre-2000, nss-sulfate shows a consistent decline in each season with the weakest decline in winter and the strongest reduction measured in JJA at -0.036 $\mu$g m$^{-3}$yr$^{-1}$ (R$^2$=0.72, Table 1). Post-2000, nss-sulfate increased during every season with comparable increases in every season. In JJA, nss-sulfate increased at +0.028 $\mu$g m$^{-3}$yr$^{-1}$ (R$^2$=0.61, Table 1). In contrast, nitrate shows no trend (e.g., R$^2$<0.2) in any season except a slight increase of +0.012 $\mu$g m$^{-3}$yr$^{-1}$ post-2000 in JJA. Unlike nitrate which showed intermittent spikes associated with increased biomass burning aerosol transport

14

391    periods, the persistent increases in nss-sulfate observed during all seasons more likely reflect either
392    increased emissions or more efficient oxidation of $SO_2$.

393    **Table 1:** Seasonal trends in nitrate and nss-sulfate shown pre- and post-2000. The rate of change in $\mu g/m^3/yr$
394        is shown and the correlation coefficient is also included. Values of $R^2<0.2$ were denoted as having
395        "No Trend". DJF represents winter, MAM represents spring, JJA represents summer, and SON
396        represents fall.

| Season | Compound | Pre-2000 Rate of Change ($\mu g/m^3/yr$) | Post-2000 Rate of Change ($ug/m^3/yr$) |
|--------|----------|----------------------------|----------------------------|
| DJF | Nitrate | -0.0005 (R2=0.05, No Trend) | +0.013 (R2=0.07, No Trend) |
|  | NSS-Sulfate | -0.0070 (R2=0.05, No Trend) | +0.035 (R2=0.48) |
| MAM | Nitrate | +0.0037 (R2=0.01, No Trend) | +0.028 (R2=0.08, No Trend) |
|  | NSS-Sulfate | -0.034 (R2=0.64) | +0.033 (R2=0.09, No Trend) |
| JJA | Nitrate | -0.002 (R2=0.02, No Trend) | +0.012 (R2=0.21) |
|  | NSS-Sulfate | -0.036 (R2=0.72) | +0.028 (R2=0.61) |
| SON | Nitrate | +0.0003 (R2=0.02, No Trend) | +0.013 (R2=0.13, No Trend) |
|  | NSS-Sulfate | -0.023 (R2=0.29) | +0.026 (R2=0.44) |

399    Figure 6 compares yearly trends in Ragged Point nss-sulfate along with $SO_2$ emissions reported
400    from the Community Emissions Data System (CEDS) (McDuffie et al., 2020). We focus on the
401    most likely sources to impact Ragged Point: the U.S., EU, and Africa. A similar figure comparing
402    nitrate concentrations measured at Ragged Point and nitrogen dioxide ($NO_2$) emissions from
403    CEDS can be found in the SI (Fig S6). Our near-constant nitrate mass concentrations do not match
404    the decline in $NO_2$ observed in the EU and U.S. and the increase in $NO_2$ in Africa. In contrast,
405    decreases in nss-sulfate observed from 1990-2000 at Ragged Point closely follow the 32% and
406    58% reductions of $SO_2$ emissions in the U.S. and Europe, respectively (Fig 6) (Aas et al., 2019;
407    Hand et al., 2012; McDuffie et al., 2020; Rafaj et al., 2015; Yang et al., 2020). Our finding that
408    changing $SO_2$ emissions in the EU and U.S. is reflected in our record at Ragged Point agrees with
409    previous work examining both anthropogenic and biogenic sulfate (Savoie et al., 2002). Figure 6
410    also compares the trends of nss-sulfate observed at Ragged Point to increasing emissions of $SO_2$
411    from Africa (McDuffie et al., 2020). Before 2000, $SO_2$ emissions from Africa oscillated around
412    4.44±0.19 Tg S/yr but show no consistent trend ($R^2$=0.027). However, after 2000, emissions of
413    $SO_2$ from Africa steadily increase by 37% from 2000-2011 (4.33 Tg S/yr in 2000 and 5.95 Tg S/yr
414    in 2011, $R^2$=0.88). The rate of increase in $SO_2$ is on par with the rate of increase in nss-sulfate of
415    29% observed in Barbados suggesting that anthropogenic emissions from Africa are affecting the
416    nss-sulfate trends measured in Barbados.

417    We next utilized the CMAQ model results from EQUATES to gain further insight into the
418    observed recovery of nss-sulfate (post-2000). We first note that EQUATES also predicts an
419    increase in $SO_2$ emissions from northern hemispheric Africa after 2002 (see Figure S7). However,
420    we use EQUATES to determine if other factors such as changes in the oxidation efficiency of
421    locally emitted $SO_2$ and meteorological changes affected our observations.

15
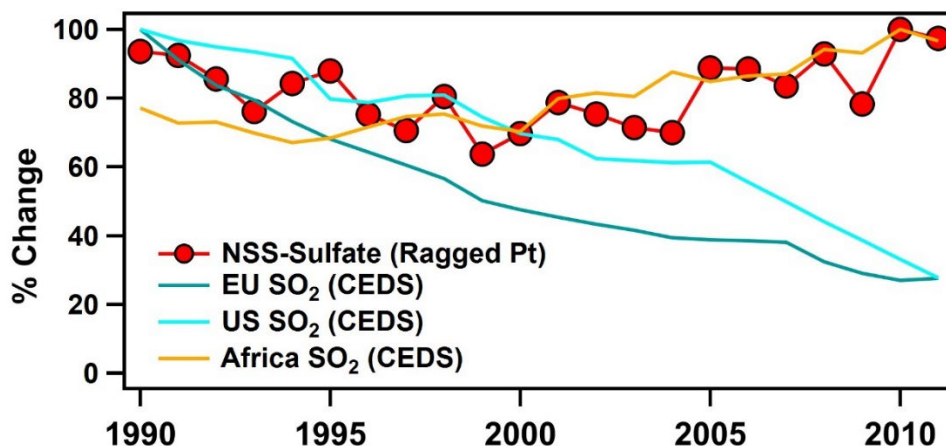
**Figure 6:** Percent changes in NSS-Sulfate mass concentrations measured at Ragged Point from 1990-2011 are shown in red. NSS-Sulfate mass decreases from 0.87 µg/m$^3$ in 1990 to 0.64 µg/m$^3$ in 2000 and subsequently increases to 0.90 µg/m$^3$ in 2011. The data are normalized to the maximum NSS-sulfate mass concentration, 0.92 µg/m$^3$ measured in 2010. The percent changes in emissions of sulfur dioxide (SO$_2$) from the CEDS emissions inventory from McDuffie et al., 2020 are included for comparison. Decreasing emissions of SO$_2$ from the U.S. and EU are shown in blue lines. U.S. SO$_2$ reduces from 21.12 to 5.85 Tg S/yr and EU SO$_2$ reduces from 28.06 to 7.74 Tg S/yr. Percentages are calculated by normalizing to the maximum values in SO$_2$ emissions observed in 1990 for both the U.S. and EU. SO$_2$ emissions from Africa increased from 4.13 to 5.95 Tg S/yr; they are normalized to the maximum SO$_2$ emissions observed in 2010 at 6.16 Tg S/yr.

## 3.2 Comparison of Measured and Modeled Trends of Nitrate and Sulfate Aerosol

Monthly concentrations of simulated nss-sulfate and nitrate (for both the fine and coarse mode combined) were compared with mass concentrations measured on filters collected at Ragged Point (see Fig 7 and 8, respectively). The model simulates similar concentrations both at Ragged Point and the area to the east of the site implying that emissions on Barbados are minimal. EQUATES predicts nitrate concentrations in fine and coarse aerosol sizes. A greater proportion of fine nitrate is predicted in DJF (40% of the total modeled nitrate) and MAM (26% of the total modeled nitrate) during all years compared to JJA and SON (18% of the total modeled nitrate for both seasons, see Fig S8). This seasonality is likely due to increased contributions of nitrate from fine biomass-burning aerosol produced in Sub-Saharan Africa north of the equator in winter and spring. This point is highlighted in MAM of 2010 when the amount of modeled fine nitrate was elevated (35% of total modeled nitrate). Nss-sulfate is predicted to be almost exclusively in fine mode aerosol. While previous observations have shown that nss-sulfate dominates the fine mode in Barbados, some of the nss-sulfate is also present in the coarse mode likely due to heterogeneous reactions between SO$_2$ and coarse sea spray and mineral dust aerosols (Adams et al., 2005; Alexander et al., 2005; Li-Jones & Prospero, 1998). EQUATES does not seem to be capturing this minor yet important budget of nss-sulfate.

16
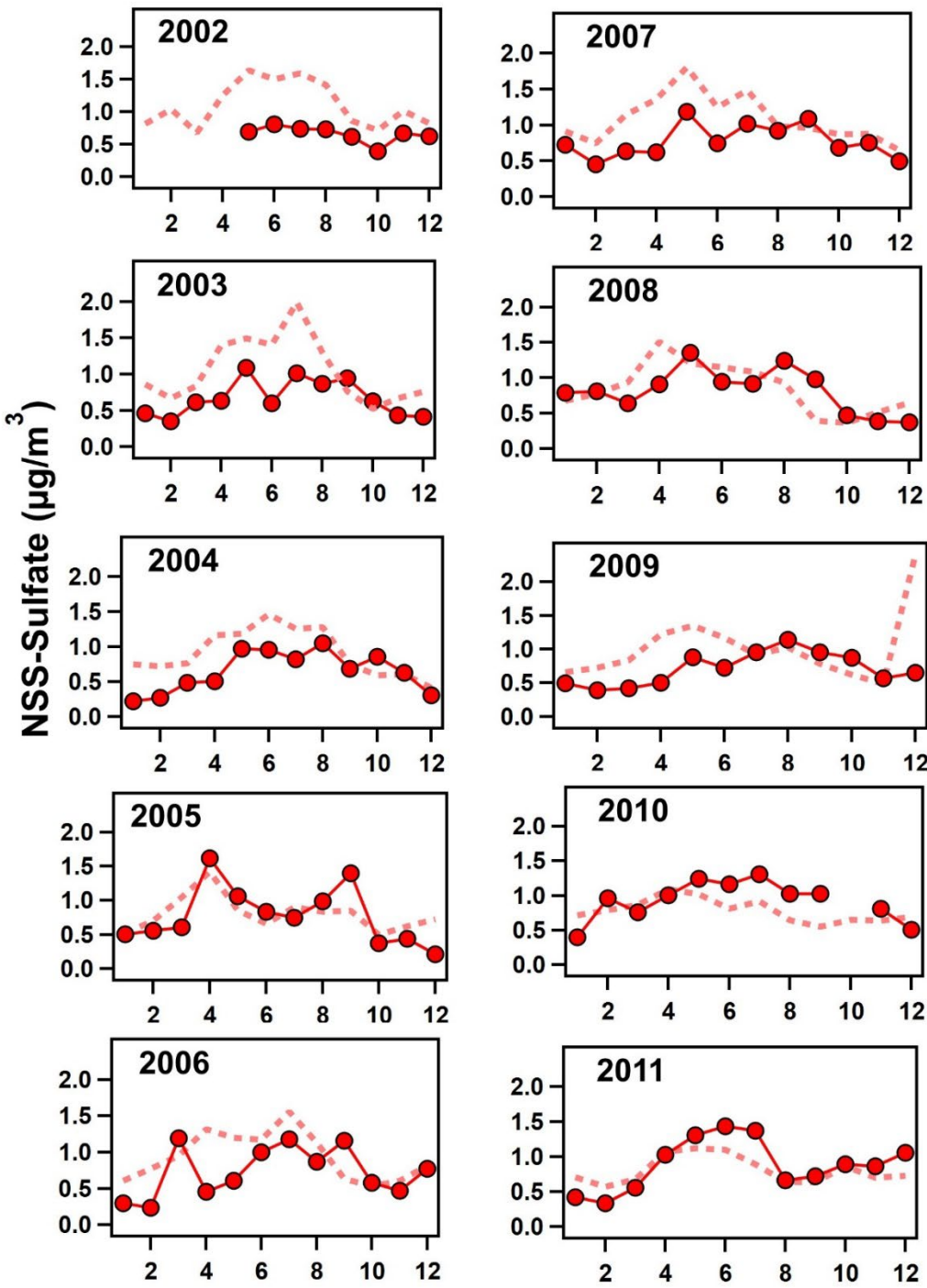
451
**Figure 7:** Monthly averages of non-sea salt sulfate (nss-sulfate) mass concentrations measured at Barbados
on filters (solid red line with red circles) compared to monthly averages of NSS-sulfate calculated from
EQUATES model simulations of combined fine and coarse mode sodium (Na) and sulfate using equation
2 (dashed red line) for 2002-2011.
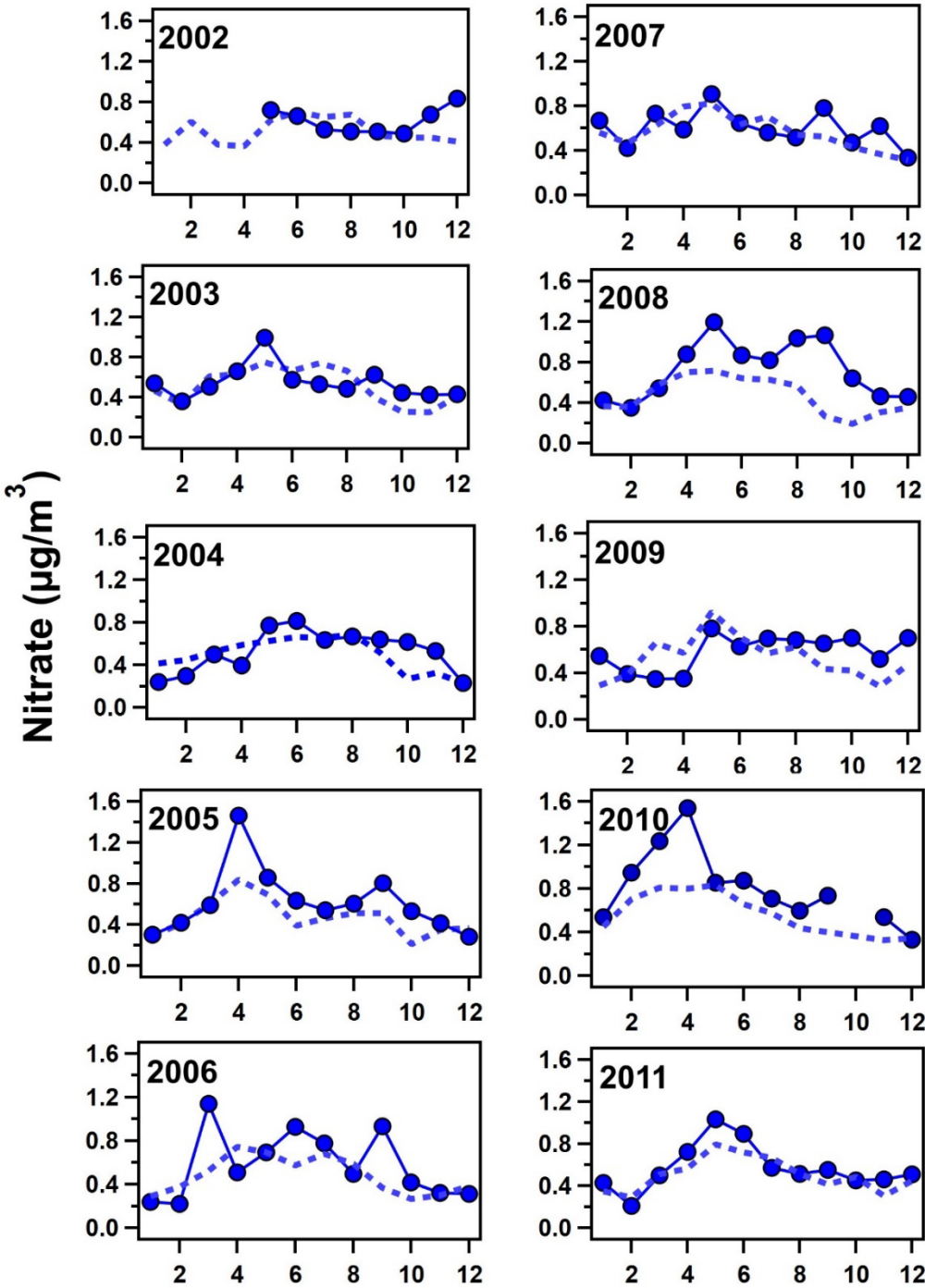
**Figure 8:** Monthly averages of nitrate mass concentrations measured in Barbados on filters (solid blue line with blue circles) compared to monthly averages of combined fine and coarse mode nitrate calculated from EQUATES model simulations (dashed blue line) for 2002-2011.
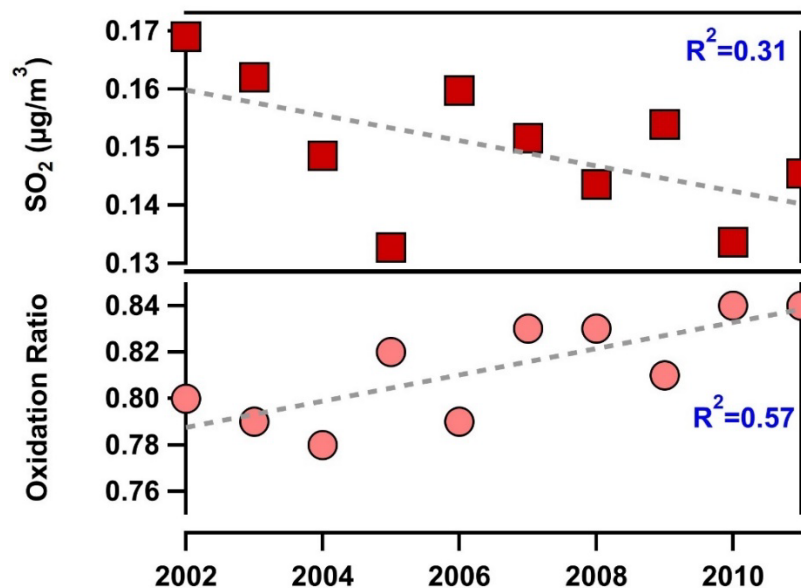
To assess the performance of the model compared to our observations, we calculated the normalized mean bias (NMB) and Pearson correlation coefficient (r) for monthly averaged concentrations of nss-sulfate and nitrate (see Table S1 (Boylan & Russell, 2006)). Additional calculations of the mean bias (MB) and root-mean-square error (RMSE) can also be found in Table S1 of the SI. NMB for nitrate was generally within ±20%, better than predictions of nitrate within the U.S. (Kelly et al., 2019), except for 2005 (-24.18%) as well as 2008 (-35.06%) and 2010 (-28.72%) when the model underpredicted measurements likely due to the elevated African smoke transport events. The model overpredicts nss-sulfate in the earlier years (2002-2007) then converges closer to our measurements at Ragged Point after 2008 as shown in Fig 7. Because trends in sea salt (e.g., sodium from EQUATES, Figure S1) show a constant high bias in all years, the overprediction of nss-sulfate reflects biases in sources of sulfate (other than sea spray) or biases in the conversion of $SO_2$ to sulfate. Further, the NMB for nss-sulfate also reflects the model overprediction of nss-sulfate as high values are observed in 2002 (+81.45%) then the model begins to fall within ±20% starting in 2008 (see Table S1). As such, trends in nss-sulfate simulated by EQUATES show a decrease over time rather than an increase post-2000 (see Fig S9). The decrease in EQUATES simulations of nss-sulfate post-2000 compared to the increase observed in Barbados could be related to a changing bias over time. For example, recent predictions for 2019 indicate CMAQ underpredicts sulfate by about 50% in the eastern U.S. (45% underestimate across entire U.S.) (Vannucci et al., 2024). Previous simulations for 2002 and 2016 indicated more modest normalized mean biases of 20% or less (Appel et al., 2021; Sarwar et al., 2011). As a result, EQUATES may simulate a stronger decline in transported U.S. sulfate over 2002-2019 than observations indicate. This overestimate in declining sulfate in the U.S. may mask trends (including stronger increases in sulfate) in other regions. Pearson correlation coefficients range from -0.22 to 0.88 by year for nitrate with a mean of 0.54. The poorest correlation (-0.22) occurs for 2002 when Barbados filter measurements were unavailable from January until May. For nss-sulfate, r ranges from 0.23 to 0.82 by year with a mean of 0.59. The greatest variation between the model and measurements is for 2009 (see Fig 7), which was also the year that had an erroneously high model concentration of sea spray aerosol in winter. Overall, the model is capturing both the magnitude and seasonal and interannual variation of nss-sulfate and nitrate at our remote location in the tropical North Atlantic.

### 3.2.1 Using EQUATES to Determine Contributions to Aerosol Sulfate

Figure 9 shows a decrease in $SO_2$ simulated by EQUATES within the modeled grid space over Ragged Point and to the east of the site. Consistent with a predicted decrease in $SO_2$ and the observed increase in nss-sulfate, the oxidation ratio of $SO_2$ increases in the region near Barbados. We note that because the lifetime of $SO_2$ is predicted to be ~20 hours and as much as ~40 hours depending on the latitude of the source of $SO_2$ and the season (Green et al., 2019; Lee et al., 2011), our oxidation ratio estimates here are most relevant for local emissions, including sulfur emitted from marine phytoplankton (e.g., DMS). However, prior measurements at Bermuda suggest a longer lifetime for long-range transported $SO_2$ compared to local oceanic emissions from DMS, which are subject to strong condensational losses to sea spray in the marine boundary layer (Keene et al., 2014). As such, long-range transported sources from Africa, the U.S., and EU have likely been converted to sulfate upwind of Barbados and $SO_2$ concentrations shown here most likely

**Figure 9:** Annual trends in locally emitted sulfur dioxide ($SO_2$) simulated by the EQUATES model and the
calculated oxidation ratio at Ragged Point. Linear fits and corresponding correlation coefficients are also
shown.



20
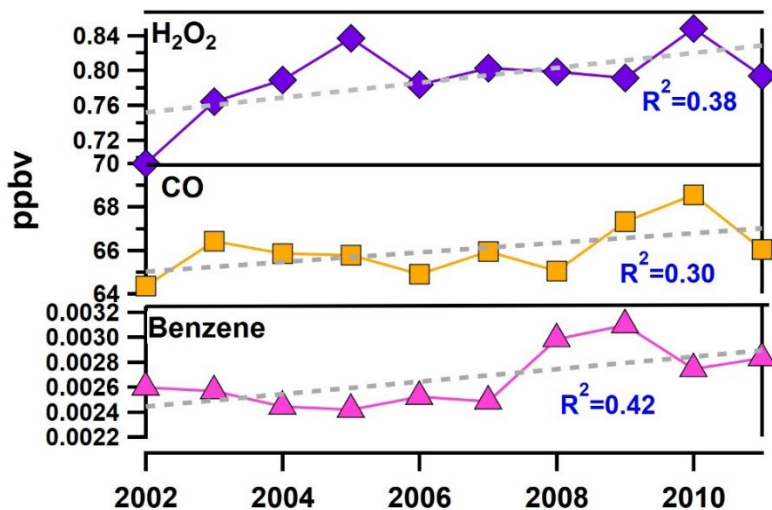
**Figure 10:** Annual trends in select gas phase species including benzene (pink trace, bottom panel), carbon monoxide (CO) (orange trace, middle panel), and hydrogen peroxide ($H_2O_2$) (purple trace, top panel) simulated by the EQUATES model at Ragged Point. Linear fits and corresponding correlation coefficients are also shown.

Changes in biomass burning, anthropogenic emissions, oxidant concentrations, and meteorological parameters were also investigated using EQUATES. Fine mode non-sea salt potassium (nss-$K^+$) was used as our tracer for smoke emissions. We used EQUATES data rather than our nss-$K^+$ observations, which were non-existent for most years from 2002-2011. Also, our measurements included total (i.e., fine and coarse mode) nss-$K^+$ including contributions from African dust (Savoie & Prospero, 1980). EQUATES simulations of nss-K+ were a factor of 2-3 higher than our measurements except for the dust and smoke transport event that occurred in MAM of 2010. No significant increase in simulated nss-$K^+$ was estimated (Fig S10). Meteorological parameters (temperature, relative humidity (RH), wind speed, wind direction) were constant over time showing no shift in rainfall, winds, temperature, or RH (Fig S10). Concentrations of the hydroxyl radical ($^{\bullet}OH$) did not show a significant change from 2002-2011 (Fig S10). EQUATES concentrations of benzene (a tracer for fossil fuel combustion) and carbon monoxide (CO, a tracer for combustion from fossil fuels and biomass burning) both increased modestly from 2002-2011 (Fig 10). Our results suggest that an increase in the oxidation efficiency of locally emitted $SO_2$ to sulfate may contribute to the increase of nss-sulfate post-2000, but the contribution is likely small compared to long-range transported sulfate.

## 4. DISCUSSION & CONCLUSIONS

Our 21-year record (1990-2011) of nitrate and nss-sulfate aerosol shows two distinct trends over the tropical North Atlantic. Nitrate shows no significant change other than two spikes in JJA and September of 2008 and MAM of 2010. Variations in winter- and spring-time dust transport explained interannual oscillations in nitrate concentrations while increased transport of smoke from Sub-Saharan Africa north of the equator in MAM 2010 and from south of the equator and, possibly, South America in September 2008 caused the increased levels of nitrate observed in those years. Nitrate has been shown to be enhanced in smoke by up to 5-fold over background due to high emissions of $NO_x$ that are rapidly converted to nitrate (Adon et al., 2010; Hickman et al., 2021; Perron et al., 2022; Schlosser et al., 2017). Notably, nitrate was not enhanced in JJA of 2010 even though high quantities of dust were transported to Barbados. We speculate that the lack of enhanced nitrate during summer of 2010 is due to the lack of nitrate contribution from African smoke emissions during this season. This finding in addition to our observations of enhanced nitrate associated with dust in DJF and MAM suggests that the nitrate associated with African aerosol transport primarily originates from $NO_x$ emissions from African wildfires that are rapidly converted to nitrate prior to transport.

In contrast to the relatively flat trend in aerosol nitrate, nss-sulfate decreased by 30% from 1990-2000 then increased from 2000-2011, recovering to concentrations measured in the early 1990s. Reductions in nss-sulfate observed in Barbados are most likely due to decreased emissions of $SO_2$ in the U.S. and EU due to clean air policies implemented via technologies such as flue-gas desulfurization devices installed in power plants (Aas et al., 2019; Kharol et al., 2017; Smith et al.,

21

560 2011). Thus, our results highlight that regulations aimed to improve national and regional air
561 quality also impact more distant locations such as the remote North Atlantic marine boundary layer
562 and Caribbean.

563      As shown in Fig 6, increases in $SO_2$ in Africa, namely from anthropogenic sources, are the
564 most probable cause for the increase in nss-sulfate levels from 2000-2011 in Barbados.
565 Simulations from both CEDS and EQUATES reveal an increase in anthropogenic emissions of
566 $SO_2$. Further evidence for this speculation stems from the lack of change in air mass back
567 trajectories before and after 2000, suggesting that emissions rather than meteorological trends are
568 driving our observed patterns in nss-sulfate. Industrial contributions of sulfate from oil refineries,
569 coal fired power plants, and fertilizer plants along the north and northwestern coast of Africa were
570 also observed in the Cape Verde Islands (Salvador et al., 2015). Anthropogenic sources of $SO_2$ in
571 Africa include emissions from electricity generation, diesel combustion and transportation
572 (Assamoi & Liousse, 2010; Keita et al., 2021; Liousse et al., 2014), refineries, gas flaring, and
573 smelting (Doumbia et al., 2019; Osuji & Avwiri, 2005). Levels of pollution in African cities are
574 on par with Asian megacities with the largest rate of increases in $SO_2$ observed in western Africa
575 (Adon et al., 2016; Hopkins et al., 2009; Liousse et al., 2014; Val et al., 2013). The industrial sector
576 in the Highveld region of South Africa also shows some of the highest increases in $SO_2$ with
577 observed increases starting in 1980 due to an increase in the number of coal-fired power plants
578 arising from an increased demand for electricity (Keita et al., 2021; Liousse et al., 2014;
579 Shikwambana et al., 2020). From 1990-2011, the CEDS inventory shows the largest increase in
580 $SO_2$ emissions in Africa starting in 2000, coincident with the increase in nss-sulfate observed at
581 our site (see Figure 6). The emissions inventory for Africa is also likely underestimated due to a
582 lack of measurements (McDuffie et al., 2020). Therefore, we speculate that anthropogenic $SO_2$
583 emissions are likely higher than shown from the CEDS model and are driving the observed
584 increases in nss-sulfate in Barbados.

585      In addition to sources of $SO_2$ within Africa, $SO_2$ emissions from other nearby countries and
586 regions have been shown to be exported to Africa (Koch et al., 2007). In particular, $SO_2$ emissions
587 in India have rapidly risen and overtaken China as the largest emitter of $SO_2$ (Li et al., 2017) while
588 remote sensing observations have highlighted that $SO_2$ emitted from oil and gas operations in the
589 Persian Gulf have been greatly underestimated in emissions inventories (McLinden et al., 2016).
590 While it is possible that these two regions may also contribute to the increase in nss-sulfate
591 observed at our measurement site, we can only speculate of their importance to the remote North
592 Atlantic marine boundary layer.

593      While some of the increases in nss-sulfate after 2000 could be due, in part, to marine
594 biogenic, shipping, biomass burning, and volcanic emissions, their contributions are likely not the
595 dominant cause of the observed trends. Marine biogenic sulfate is estimated to contribute up to
596 50% of nss-sulfate at Ragged Point during non-dust transport conditions (Li-Jones & Prospero,
597 1998; Royer et al., 2023; Savoie et al., 2002). However, our predictions of nss-sulfate and $SO_2$
598 concentrations with EQUATES includes DMS chemistry that does not explain our observed
599 trends. In fact, locally emitted $SO_2$, most likely from the ocean, is simulated to be decreasing from
600 2002-2011. Further, while recent studies have shown links between climate change and increased

22

DMS emissions at high latitudes, these trends have not been demonstrated at lower latitudes. Instead, DMS is predicted to decrease with increasing temperature at low latitudes due to stratification (Kloster et al., 2007) and increasing ocean acidification (Zhao et al., 2024) while a recent modeling study, factoring in changes in phytoplankton dynamics, found that DMS emissions have not appreciably changed from the preindustrial to the present-day (Wang et al., 2018). As such, DMS emissions do contribute to the sulfate burden but likely do not explain the recent increases in sulfate, which would also agree with findings in Bermuda where changes in the nss-sulfate burden were explained by anthropogenic rather than biogenic emissions (Keene et al., 2014). Shipping emissions likely do not explain our trends in nss-sulfate because Barbados is somewhat isolated from proximal shipping impacts—heavy shipping is concentrated in the Caribbean west of Barbados and along the north coast of South America (Czermański et al., 2021). Biomass burning has declined in northern Sub-Saharan Africa starting in the early 2000s (Andela et al., 2017; Andela & Van Der Werf, 2014; Zubkova et al., 2019). Further, increased nss-sulfate has been observed year-round rather than just during the main burn seasons, suggesting that this source alone is likely not responsible for the major increases in nss-sulfate observed at our site. The largest natural source of $SO_2$ in Africa is volcanic emissions from Mount Nyiragongo in the Goma region of the Democratic Republic of Congo, which has been shown to impact sulfate aerosol at the Amazon Tall Tower Observatory (ATTO) in Brazil (Opio et al., 2021; Saturno et al., 2018). Volcanic emissions likely do impact nss-sulfate measured in Barbados but there is no evidence that emissions from this source are increasing. These lines of evidence further support an anthropogenic source as the cause of the increase in nss-sulfate observed in Barbados.

In addition to increased sulfate transported from Africa, the oxidation ratio was simulated to increase from 2002-2011, which would more efficiently convert locally emitted $SO_2$ to sulfate and may represent a minor addition to the budget of nss-sulfate. Further, concentrations of $H_2O_2$ increased in the post-2000 period indicating a potential increase in the efficiency of aqueous phase oxidation. We would expect that even if the total burden of $SO_2$ has been reduced globally (McDuffie et al., 2020; Smith et al., 2011), $SO_2$ emitted locally is more efficiently converted to sulfate due to greater availability of oxidants at lower latitudes (Manktelow et al., 2007). It is important to note, however, that the oxidation ratio calculated is most appropriate for accounting for changing oxidation efficiencies of $SO_2$ and sulfate formation near the site, and the oxidation ratio does not account for changes in the oxidation efficiency of already formed sulfate aerosol that has been transported to the site. For example, $SO_2$ emitted from Africa is likely already oxidized to sulfate prior to being transported to our site.

One question that persists is why nitrate did not increase from 2000-2011 alongside the increase in nss-sulfate? One possible explanation is a combination of reduced $NO_x$ from smoke concurrent with increased dust and smoke transport that offset any changes in nitrate other than the observed spikes in 2008 and 2010. In the 2000s, biomass burning emissions declined in northern equatorial Africa due to a combination of increased precipitation in DJF associated with a shift from more frequent El Niño events in the 1990s to more frequent La Niña events in the 2000s and land use practices converting tropical savanna to cropland (Andela et al., 2017; Andela & Van Der Werf, 2014; Hickman et al., 2021; Zubkova et al., 2019). The recently updated Barbados dust record highlights that dust is being transported to the Caribbean earlier in the year

643 and arriving more frequently in spring (Zuidema et al., 2019), which would increase the transport
644 of biomass burning emissions and associated nitrate to the Caribbean and remote North Atlantic,
645 which may effectively cancel out the impact of reduced smoke emissions.

646       The Ragged Point site in Barbados has historically been associated with research on
647 African dust transport (Prospero et al., 2021). However, this work highlights that the site is also
648 an excellent indicator of long-term and large-scale changes in emissions and the impact of air
649 quality policies or the lack of them or poor compliance to them. Looking forward, building upon
650 the existing time series of nitrate and sulfate aerosol while also expanding the measurement
651 capabilities at Ragged Point to incorporate measurements of metals, which will increase our ability
652 to apportion aerosol sources, and carbonaceous aerosol will provide needed insight into the impact
653 of anthropogenic and biomass burning on sulfate and nitrate burdens over the remote North
654 Atlantic that complement recent work performed in the South Atlantic (Zuidema et al., 2016,
655 2018).

656

663

664 **Author Contribution:** CJG analyzed measurement and model data and wrote the manuscript.
665 JMP, LC, EB, PS collected data, operated the site, and analyzed filters for dust, sea salt, sulfate
666 and nitrate mass concentrations. KF and HOTP provided EQUATES model simulations and helped
667 with their interpretation. JAC performed HYSPLIT analysis. All authors read and edited the
668 manuscript.

669

670 **Competing Interests:** The authors declare that they have no conflict of interest.

671

672 **Disclaimer:** The views expressed in this paper are those of the authors and do not necessarily
673 represent the views or policies of the US Environmental Protection Agency.

674

authors acknowledge the contributions of Dennis L. Savoie for his efforts to measure soluble ions and dust mass concentrations from the AEROCE network. We thank Wyat Appel, Kathleen Fahey, and Jeff Willison for helpful comments that improved the quality of this manuscript. We thank two anonymous reviewers for thoughtful reviews that improved this manuscript.

## REFERENCES CITED

Aas, W., Mortier, A., Bowersox, V., Cherian, R., Faluvegi, G., Fagerli, H., Hand, J., Klimont, Z., Galy-Lacaux, C., Lehmann, C. M. B., Myhre, C. L., Myhre, G., Olivié, D., Sato, K., Quaas, J., Rao, P. S. P., Schulz, M., Shindell, D., Skeie, R. B., Stein, A., Takemura, T., Tsyro, S., Vet, R., & Xu, X. (2019). Global and regional trends of atmospheric sulfur. *Scientific Reports 2019 9:1*, *9*(1), 1–11. https://doi.org/10.1038/s41598-018-37304-0

Adams, A. M., Prospero, J. M., & Zhang, C. D. (2012). CALIPSO-derived three-dimensional structure of aerosol over the Atlantic Basin and adjacent continents. *Journal of Climate*, *25*(19), 6862–6879.

Adams, J. W., Rodriguez, D., & Cox, R. A. (2005). The uptake of $SO_2$ on Saharan dust: A flow tube study. *Atmospheric Chemistry and Physics*, *5*(10), 2679–2689. https://doi.org/10.5194/ACP-5-2679-2005

Adams, P. J., Seinfeld, J. H., & Koch, D. M. (1999). Global concentrations of tropospheric sulfate, nitrate, and ammonium aerosol simulated in a general circulation model. *Journal of Geophysical Research: Atmospheres*, *104*(D11), 13791–13823. https://doi.org/10.1029/1999JD900083

Adebiyi, A. A., & Zuidema, P. (2016). The role of the southern African easterly jet in modifying the southeast Atlantic aerosol and cloud environments. *Quarterly Journal of the Royal Meteorological Society*, *142*(697), 1574–1589.

Adon, M., Galy-Lacaux, C., Yoboué, V., Delon, C., Lacaux, J. P., Castera, P., Gardrat, E., Pienaar, J., Al Ourabi, H., Laouali, D., Diop, B., Sigha-Nkamdjou, L., Akpo, A., Tathy, J. P., Lavenu, F., & Mougin, E. (2010). Long term measurements of sulfur dioxide, nitrogen dioxide, ammonia, nitric acid and ozone in Africa using passive samplers. *Atmospheric Chemistry and Physics*, *10*(15), 7467–7487. https://doi.org/10.5194/ACP-10-7467-2010

Adon, M., Yobou, V., Galy-Lacaux, C., Liousse, C., Diop, B., Hadji, E., Doumbia, T., Gardrat, E., Ndiaye, S. A., & Jarnot, C. (2016). Measurements of $NO_2$, $SO_2$, $NH_3$, $HNO_3$ and $O_3$ in West African urban environments. https://doi.org/10.1016/j.atmosenv.2016.03.050

Alexander, B., Park, R. J., Jacob, D. J., Li, Q. B., Yantosca, R. M., Savarino, J., Lee, C. C. W., & Thiemens, M. H. (2005). Sulfate formation in sea-salt aerosols: Constraints from oxygen isotopes. *Journal of Geophysical Research: Atmospheres*, *110*(D10), 1–12. https://doi.org/10.1029/2004JD005659

Andela, N., Morton, D. C., Giglio, L., Chen, Y., Van Der Werf, G. R., Kasibhatla, P. S., DeFries, R. S., Collatz, G. J., Hantson, S., Kloster, S., Bachelet, D., Forrest, M., Lasslop, G., Li, F.,

Mangeon, S., Melton, J. R., Yue, C., & Randerson, J. T. (2017). A human-driven decline in global burned area. *Science*, *356*(6345), 1356–1362. https://doi.org/10.1126/science.aal4108

Andela, N., & Van Der Werf, G. R. (2014). Recent trends in African fires driven by cropland expansion and El Niño to La Niña transition. https://doi.org/10.1038/NCLIMATE2313

Andreae, M. O., Ferek, R. J., Bermond, F., Byrd, K. P., Engstrom, R. T., Hardin, S., Houmere, P. D., LeMarrec, F., & Raemdonck, H. (1985). Dimethyl sulfide in the marine atmosphere. *Journal of Geophysical Research*, *90*(D7), 12891–12900.

Andreae, M. O. (1983). Soot Carbon and Excess Fine Potassium: Long-Range Transport of Combustion-Derived Aerosols. *Science*, *220*(4602), 1148–1151. https://doi.org/10.1126/SCIENCE.220.4602.1148

Andreae, M. O. (2019). Emission of trace gases and aerosols from biomass burning - An updated assessment. *Atmospheric Chemistry and Physics*, *19*(13), 8523–8546. https://doi.org/10.5194/ACP-19-8523-2019

Andreae, M.O., & Merlet, P. (2001). Emission of trace gases and aerosols from biomass burning. *Global Biogeochemical Cycles*, *15*(4), 955–966.

Appel, B. R., Kothny, E. L., Hoffer, E. M., Hidy, G. M., & Wesolowski, J. J. (1978). Sulfate and nitrate data from California Aerosol Characterization Experiment (ACHEX). *Environmental Science & Technology*, *12*(4), 418–425.

Appel, K. W., Bash, J. O., Fahey, K. M., Foley, K. M., Gilliam, R. C., Hogrefe, C., Hutzell, W. T., Kang, D., Mathur, R., Murphy, B. N., Napelenok, S. L., Nolte, C. G., Pleim, J. E., Pouliot, G. A., Pye, H. O. T., Ran, L., Roselle, S. J., Sarwar, G., Schwede, D. B., Sidi, F. I., Spero, T. L., & Wong, D. C. (2021). The Community Multiscale Air Quality (CMAQ) model versions 5.3 and 5.3.1: system updates and evaluation. *Geosci. Model Dev*, *14*, 2867–2897. https://doi.org/10.5194/gmd-14-2867-2021

Assamoi, E. M., & Liousse, C. (2010). A new inventory for two-wheel vehicle emissions in West Africa for 2002. *Atmospheric Environment*, *44*(32), 3985–3996. https://doi.org/10.1016/J.ATMOSENV.2010.06.048

Barkley, A. E., Prospero, J. M., Mahowald, N., Hamilton, D. S., Popendorf, K. J., Oehlert, A. M., Pourmand, A., Gatineau, A., Panechou-Pulcherie, K., Blackwelder, P., & Gaston, C. J. (2019). African biomass burning is a substantial source of phosphorus deposition to the Amazon, Tropical Atlantic Ocean, and Southern Ocean. *Proceedings of the National Academy of Sciences of the United States of America*, *116*(33), 16216–16221. https://doi.org/10.1073/pnas.1906091116

Barkley, A. E., Olson, N. E., Prospero, J. M., Gatineau, A., Panechou, K., Maynard, N. G., Blackwelder, P., China, S., Ault, A. P., & Gaston, C. J. (2021). Atmospheric transport of North African dust-bearing supermicron freshwater diatoms to South America: Implications for iron transport to the equatorial North Atlantic Ocean. *Geophysical Research Letters*, *48*(5), e2020GL090476. https://doi.org/10.1029/2020GL090476

Barnes, I., Hjorth, J., & Mihalopoulos, N. (2006). Dimethyl sulfide and dimethyl sulfoxide and their oxidation in the atmosphere. *Chemical Reviews*, *106*(3), 940–975.

Benish, S. E., Bash, J. O., Foley, K. M., Appel, K. W., Hogrefe, C., Gilliam, R., & Pouliot, G. (2022). Long-term regional trends of nitrogen and sulfur deposition in the United States from 2002 to 2017. *Atmospheric Chemistry and Physics*, *22*(19), 12749–12767. https://doi.org/10.5194/ACP-22-12749-2022

Boylan, J. W., & Russell, A. G. (2006). PM and light extinction model performance metrics, goals, and criteria for three-dimensional air quality models. *Atmospheric Environment*, *40*, 4946–4959. https://doi.org/10.1016/j.atmosenv.2005.09.087

Carlson, T. N., & Prospero, J. M. (1972). The large-scale movement of Saharan air outbreaks over the Northern Equatorial Atlantic. *Journal of Applied Meteorology*, *aa*(2), 283–297.

Carslaw, K. S., Lee, L. A., Reddington, C. L., Pringle, K. J., Rap, A., Forster, P. M., Mann, G. W., Spracklen, D. V., Woodhouse, M. T., Regayre, L. A., & Pierce, J. R. (2013). Large contribution of natural aerosols to uncertainty in indirect forcing. *Nature*, *503*, doi:10.1038/nature12674.

Charlson, R. J., Schwartz, S. E., Hales, J. M., Cess, R. D., Coakley, J. A., Hansen, J. E., & Hofmann, D. J. (1992). Climate forcing by anthropogenic aerosols. *Science*, *255*(5043), 423–430. https://doi.org/10.1126/SCIENCE.255.5043.423

Chiapello, I., Moulin, C., & Prospero, J. M. (2005). Understanding the long-term variability of African dust transport across the Atlantic as recorded in both Barbados surface concentrations and large-scale Total Ozone Mapping Spectrometer (TOMS) optical thickness. *Journal of Geophysical Research: Atmospheres*, *110*(D18), 1–9. https://doi.org/10.1029/2004JD005132

Czermański, E., Cirella, G. T., Notteboom, T., Oniszczuk-Jastrzabek, A., & Pawłowska, B. (2021). An energy consumption approach to estimate air emission reductions in container shipping. *Energies 2021, Vol. 14, Page 278*, *14*(2), 278. https://doi.org/10.3390/EN14020278

Doherty, O. M., Riemer, N., & Hameed, S. (2008). Saharan mineral dust transport into the Caribbean: Observed atmospheric controls and trends. *Journal of Geophysical Research: Atmospheres*, *113*(D7). https://doi.org/10.1029/2007JD009171

Doherty, O. M., Riemer, N., & Hameed, S. (2012). Control of Saharan mineral dust transport to Barbados in winter by the Intertropical Convergence Zone over West Africa. *Journal of Geophysical Research: Atmospheres*, *117*(D19), 19117. https://doi.org/10.1029/2012JD017767

Doumbia, E. H. T., Liousse, C., Keita, S., Granier, L., Granier, C., Elvidge, C. D., Elguindi, N., & Law, K. (2019). Flaring emissions in Africa: Distribution, evolution and comparison with current inventories. *Atmospheric Environment*, *199*, 423–434. https://doi.org/10.1016/J.ATMOSENV.2018.11.006

Draxler, R. R., & Rolph, G. D. (2011). HYSPLIT (HYbrid Single-Particle Lagrangian Integrated Trajectory) Model access via NOAA ARL READY Website (http://ready.arl.noaa.gov/HYSPLIT.php). *NOAA Air Resources Laboratory*, Silver Spring, MD.

Foley, K. M., Pouliot, G. A., Eyth, A., Aldridge, M. F., Allen, C., Appel, K. W., Bash, J. O., Beardsley, M., Beidler, J., Choi, D., Farkas, C., Gilliam, R. C., Godfrey, J., Henderson, B. H., Hogrefe, C., Koplitz, S. N., Mason, R., Mathur, R., Misenis, C., Possiel, N., Pye, H. O. T., Reynolds, L., Roark, M., Roberts, S., Schwede, D. B., Seltzer, K. M., Sonntag, D., Talgo, K., Toro, C., Vukovich, J., Xing, J., & Adams, E. (2023). 2002–2017 anthropogenic emissions data for air quality modeling over the United States. *Data in Brief*, *47*, 109022. https://doi.org/10.1016/J.DIB.2023.109022

Galloway, J. N., Townsend, A. R., Erisman, J. W., Bekunda, M., Cai, Z., Freney, J. R., Martinelli, L. A., Seitzinger, S. P., & Sutton, M. A. (2008). Transformation of the nitrogen cycle: Recent trends, questions, and potential solutions. *Science*, *320*(5878), 889–892. https://doi.org/10.1126/SCIENCE.1136674

Giglio, L, Randerson, J. T., & van der Werf, G. R. (2013). Analysis of daily, monthly, and annual burned area using the fourth-generation global fire emissions database (GFED4). *Journal of Geophysical Research-Biogeosciences*, *118*(1), 317–328.

Giglio, Louis, Csiszar, I., & Justice, C. O. (2006). Global distribution and seasonality of active fires as observed with the Terra and Aqua Moderate Resolution Imaging Spectroradiometer (MODIS) sensors. *Journal of Geophysical Research: Biogeosciences*, *111*(2). https://doi.org/10.1029/2005JG000142

Goudie, A. S., & Middleton, N. J. (2001). Saharan dust storms: nature and consequences. *Earth-Science Reviews*, *56*(1–4), 179–204. https://doi.org/10.1016/S0012-8252(01)00067-8

Green, J. R., Fiddler, M. N., Holloway, J. S., Fibiger, D. L., McDuffie, E. E., Campuzano-Jost, P., Schroder, J. C., Jimenez, J. L., Weinheimer, A. J., Aquino, J., Montzka, D. D., Hall, S. R., Ullmann, K., Shah, V., Jaeglé, L., Thornton, J. A., Bililign, S., & Brown, S. S. (2019). Rates of wintertime atmospheric $SO_2$ oxidation based on aircraft observations during clear-sky conditions over the Eastern United States. *Journal of Geophysical Research: Atmospheres*, *124*(12), 6630–6649. https://doi.org/10.1029/2018JD030086.

Gutleben, M., Groβ, S., Heske, C., & Wirth, M. (2022). Wintertime Saharan dust transport towards the Caribbean: an airborne lidar case study during EUREC[4]A. *Atmospheric Chemistry and Physics*, *22*, 7319-7330.

Hand, J. L., Schichtel, B. A., Malm, W. C., & Pitchford, M. L. (2012). Particulate sulfate ion concentration and $SO_2$ emission trends in the United States from the early 1990s through 2010. *Atmospheric Chemistry and Physics*, *12*(21), 10353–10365.

Hand, J. L., Prenni, A. J., & Schichtel, B. A. (2024). Trends in seasonal mean speciated aerosol composition in remote areas of the United States From 2000 through 2021. *Journal of*

*Geophysical Research: Atmospheres*, *129*(2), e2023JD039902. https://doi.org/10.1029/2023JD039902

Hickman, J. E., Andela, N., Tsigaridis, K., Galy-Lacaux, C., Ossohou, M., & Bauer, S. E. (2021). Reductions in $NO_2$ burden over north equatorial Africa from decline in biomass burning in spite of growing fossil fuel use, 2005 to 2017. *Proceedings of the National Academy of Sciences of the United States of America*, *118*(7). https://doi.org/10.1073/PNAS.2002579118/-/DCSUPPLEMENTAL

Hopkins, J. R., Evans, M. J., Lee, J. D., Lewis, A. C., Marsham, J. H., McQuaid, J. B., Parker, D. J., Stewart, D. J., Reeves, C. E., & Purvis, R. M. (2009). Direct estimates of emissions from the megacity of Lagos. *Atmospheric Chemistry and Physics*, *9*(21), 8471–8477. https://doi.org/10.5194/ACP-9-8471-2009

*https://gispub.epa.gov/air/trendsreport/2023/*. (2023).

Jickells, T. D., Buitenhuis, E., Altieri, K., Baker, A. R., Capone, D., Duce, R. A., Dentener, F., Fennel, K., Kanakidou, M., LaRoche, J., Lee, K., Liss, P., Middelburg, J. J., Moore, J. K., Okin, G., Oschlies, A., Sarin, M., Seitzinger, S., Sharples, J., Singh, A., Suntharalingam, P., Uematsu, M., & Zamora, L. M. (2017). A reevaluation of the magnitude and impacts of anthropogenic atmospheric nitrogen inputs on the ocean. *Global Biogeochemical Cycles*, *31*(2), 289–305. https://doi.org/10.1002/2016GB005586

Keene, W. C., Pszenny, A. A. P., Galloway, J. N., & Hawley, M. E. (1986). Sea-salt corrections and interpretation of constituent ratios in marine precipitation. *Journal of Geophysical Research*, *91*(D6), 6647. https://doi.org/10.1029/JD091ID06P06647

Keene, W. C., Moody, J. L., Galloway, J. N., Prospero, J. M., Cooper, O. R., Eckhardt, S., & Maben, J. R. (2014). Long-term trends in aerosol and precipitation composition over the western North Atlantic Ocean at Bermuda. *Atmospheric Chemistry and Physics*, *14*(15), 8119–8135.

Keita, S., Liousse, C., Assamoi, E. M., Doumbia, T., N'Datchoh, E. T., Gnamien, S., Elguindi, N., Granier, C., & Yoboué, V. (2021). African anthropogenic emissions inventory for gases and particles from 1990 to 2015. *Earth System Science Data*, *13*(7), 3691–3705. https://doi.org/10.5194/ESSD-13-3691-2021

Kelly, J. T., Koplitz, S. N., Baker, K. R., Holder, A. L., Pye, H. O. T., Murphy, B. N., Bash, J. O., Henderson, B. H., Possiel, N. C., Simon, H., Eyth, A. M., Jang, C., Phillips, S., & Timin, B. (2019). Assessing $PM_{2.5}$ model performance for the conterminous U.S. with comparison to model performance statistics from 2007-2015. *Atmos Environ*, *214*, https://doi.org/10.1016/j.atmosenv.2019.116872.

Kganyago, M., & Shikwambana, L. (2019). Assessing spatio-temporal variability of wildfires and their impact on Sub-Saharan ecosystems and air quality using multisource remotely sensed data and trend analysis. *Sustainability*, *11*, 6811, doi:10.3390/su11236811.

Kharol, S. K., Mclinden, C. A., Sioris, C. E., Shephard, M. W., Fioletov, V., Van Donkelaar, A., Philip, S., & Martin, R. V. (2017). OMI satellite observations of decadal changes in ground-level sulfur dioxide over North America. *Atmos. Chem. Phys*, *17*, 5921–5929. https://doi.org/10.5194/acp-17-5921-2017

Kloster, S., Six, K. D., Feichter, J., Maier-Reimer, E., Roeckner, E., Wetzel, P., Stier, P., & Esch, M. (2007). Response of dimethylsulfide (DMS) in the ocean and atmosphere to global warming. *Journal of Geophysical Research: Biogeosciences*, *112*(G3). https://doi.org/10.1029/2006JG000224

Koch, D., Bond, T. C., Streets, D., Unger, N., & van der Werf, G. R. (2007). Global impacts of aerosols from particular source regions and sectors. *Journal of Geophysical Research: Atmospheres*, *112*(D2), 2205. https://doi.org/10.1029/2005JD007024

Kramer, S. J., Kirtman, B. P., Zuidema, P., & Ngan, F. (2020). Subseasonal variability of elevated dust concentrations over South Florida. *Journal of Geophysical Research: Atmospheres*, *125*(6). https://doi.org/10.1029/2019JD031874

Lee, C., Martin, R. V., Van Donkelaar, A., Lee, H., Dickerson, R. R., Hains, J. C., Krotkov, N., Richter, A., Vinnikov, K., & Schwab, J. J. (2011). $SO_2$ emissions and lifetimes: Estimates from inverse modeling using in situ and global, space-based (SCIAMACHY and OMI) observations. *Journal of Geophysical Research Atmospheres*, *116*(6). https://doi.org/10.1029/2010JD014758

Lelieveld, J., & Heintzenberg, J. (1992). Sulfate cooling effect on climate through in-cloud processing of anthropogenic $SO_2$. *Science*, *258*, 117–120.

Lelieveld, J., Berresheim, H., Borrmann, S., Crutzen, P. J., Dentener, F. J., Fischer, H., Feichter, J., Flatau, P. J., Heland, J., Holzinger, R., Korrmann, R., Lawrence, M. G., Levin, Z., Markowicz, K. M., Mihalopoulos, N., Minikin, A., Ramanathan, V., De Reus, M., Roelofs, G. J., Scheeren, H. A., Sciare, J., Schlager, H., Schultz, M., Siegmund, P., Steil, B., Stephanou, E. G., Stier, P., Traub, M., Warneke, C., Williams, J., & Ziereis, H. (2002). Global air pollution crossroads over the Mediterranean. *Science*, *298*(5594), 794–799. https://doi.org/10.1126/SCIENCE.1075457/ASSET/9D6C7086-E45D-4A4D-9892-2054F591C047/ASSETS/GRAPHIC/SE4120969007.JPEG

Lelieveld, J., Hoor, P., Jöckel, P., Pozzer, A., Hadjinicolaou, P., Cammas, J. P., & Beirle, S. (2009). Severe ozone air pollution in the Persian Gulf region. *Atmospheric Chemistry and Physics*, *9*(4), 1393–1406. https://doi.org/10.5194/ACP-9-1393-2009

Li, C., McLinden, C., Fioletov, V., Krotkov, N., Carn, S., Joiner, J., Streets, D., He, H., Ren, X., Li, Z., & Dickerson, R. R. (2017). India Is overtaking China as the world's largest emitter of anthropogenic sulfur dioxide. *Scientific Reports 2017 7:1*, *7*(1), 1–7. https://doi.org/10.1038/s41598-017-14639-8

Li-Jones, X., & Prospero, J. M. (1998). Variations in the size distribution of non-sea-salt sulfate aerosol in the marine boundary layer at Barbados: Impact of African dust. *Journal of Geophysical Research-Atmospheres*, *103*(D13), 16073–16084.

Liousse, C., Assamoi, E., Criqui, P., Granier, C., & Rosset, R. (2014). Explosive growth in African combustion emissions from 2005 to 2030. *Environmental Research Letters*, *9*(3).

Mahowald, N., Scanza, R., Brahney, J., Goodale, C. L., Hess, P. G., Moore, J. K., & Neff, J. (2017). Aerosol deposition impacts on land and ocean carbon cycles. *Curr Clim Change Rep*, *3*, 16–31.

Manktelow, P. T., Mann, G. W., Carslaw, K. S., Spracklen, D. V., & Chipperfield, M. P. (2007). Regional and global trends in sulfate aerosol since the 1980s. *Geophysical Research Letters*, *34*(14), 14803. https://doi.org/10.1029/2006GL028668

Mathur, R., Xing, J., Gilliam, R., Sarwar, G., Hogrefe, C., Pleim, J., Pouliot, G., Roselle, S., Spero, T. L., Wong, D. C., & Young, J. (2017). Extending the Community Multiscale Air Quality (CMAQ) modeling system to hemispheric scales: overview of process considerations and initial applications. *Atmos. Chem. Phys*, *17*, 12449–12474. https://doi.org/10.5194/acp-17-12449-2017

McDuffie, E. E., Smith, S. J., O'Rourke, P., Tibrewal, K., Venkataraman, C., Marais, E. A., Zheng, B., Crippa, M., Brauer, M., & Martin, R. V. (2020). A global anthropogenic emission inventory of atmospheric pollutants from sector- And fuel-specific sources (1970-2017): An application of the Community Emissions Data System (CEDS). *Earth System Science Data*, *12*(4), 3413–3442. https://doi.org/10.5194/ESSD-12-3413-2020

McLinden, C. A., Fioletov, V., Shephard, M. W., Krotkov, N., Li, C., Martin, R. V, Moran, M. D., & Joiner, J. (2016). Space-based detection of missing sulfur dioxide sources of global air pollution. https://doi.org/10.1038/NGEO2724

Murphy, D. M., Cziczo, D. J., Froyd, K. D., Hudson, P. K., Matthew, B. M., Middlebrook, A. M., Peltier, R. E., Sullivan, A., Thomson, D. S., & Weber, R. J. (2006). Single-particle mass spectrometry of tropospheric aerosol particles. *Journal of Geophysical Research-Atmospheres*, *111*(D23), D23S32, doi:10.1029/2006JD007340.

Nowell, H. K., Holmes, C. D., Robertson, K., Teske, C., & Hiers, J. K. (2018). A new picture of fire extent, variability, and drought interaction in prescribed fire landscapes: Insights from Florida Government Records. *Geophysical Research Letters*, *45*(15), 7874–7884. https://doi.org/10.1029/2018GL078679

Opio, R., Mugume, I., & Nakatumba-Nabende, J. (2021). Understanding the Trend of $NO_2$, $SO_2$ and CO over East Africa from 2005 to 2020. *Atmosphere 2021, Vol. 12, Page 1283*, *12*(10), 1283. https://doi.org/10.3390/ATMOS12101283

Osuji, L. C., & Avwiri, G. O. (2005). Flared gases and other pollutants associated with air quality in industrial areas of Nigeria: An overview. *Chemistry & Biodiversity*, *2*(10), 1277–1289. https://doi.org/10.1002/CBDV.200590099

Perron, M. M. G., Meyerink, S., Corkill, M., Strzelec, M., Proemse, B. C., Gault-Ringold, M., Sanz Rodriguez, E., Chase, Z., & Bowie, A. R. (2022). Trace elements and nutrients in wildfire plumes to the southeast of Australia. *Atmospheric Research*, *270*, 106084. https://doi.org/10.1016/J.ATMOSRES.2022.106084

Prospero, J. M. (1999). Long-term measurements of the transport of African mineral dust to the southeastern United States: Implications for regional air quality. *Journal of Geophysical Research-Atmospheres*, *104*(D13), 15917–15927.

Prospero, J. M., & Mayol-Bracero, O. L. (2013). Understanding the transport and impact of African dust on the Caribbean Basin. *Bulletin of the American Meteorological Society*, *94*(9), 1329–1337.

Prospero, J. M., Glaccum, R. A., & Nees, R. T. (1981). Atmospheric transport of soil dust from Africa to South America. *Nature*, *289*, 570–572.

Prospero, J. M., Olmez, I., & Ames, M. (2001). Al and Fe in $PM_{2.5}$ and $PM_{10}$ suspended particles in South-Central Florida: The impact of the long range transport of African mineral dust.

Prospero, J. M., Collard, F.-X., Molinie, J., & Jeannot, A. (2014). Characterizing the annual cycle of African dust transport to the Caribbean Basin and South America and its impact on the environment and air quality. *Global Biogeochemical Cycles*, *29*, 757–773. https://doi.org/10.1111/1462-2920.13280

Prospero, J. M., Delany, A. C., Delany, A. C., & Carlson, T. N. (2021). The discovery of African dust transport to the western hemisphere and the Saharan Air Layer: A history. *Bulletin of the American Meteorological Society*, *102*(6), E1239–E1260. https://doi.org/10.1175/BAMS-D-19-0309.1

Quinn, P. K., Bates, T. S., Coffman, D. J., Upchurch, L. M., Johnson, J. E., Brewer, A., Baidar, S., McCoy, I. L., & Zuidema, P. (2022). Wintertime observations of tropical northwest Atlantic aerosol properties during ATOMIC: Varying mixtures of dust and biomass burning. *Journal of Geophysical Research: Atmospheres*, *127*(8), e2021JD036253. https://doi.org/10.1029/2021JD036253

Quinn, Patricia K., Thompson, E. J., Coffman, D. J., Baidar, S., Bariteau, L., Bates, T. S., Bigorre, S., Brewer, A., De Boer, G., De Szoeke, S. P., Drushka, K., Foltz, G. R., Intrieri, J., Iyer, S., Fairall, C. W., Gaston, C. J., Jansen, F., Johnson, J. E., Krüger, O. O., Marchbanks, R. D., Moran, K. P., Noone, D., Pezoa, S., Pincus, R., Plueddemann, A. J., Pöhlker, M. L., Pöschl, U., Melendez, E. Q., Royer, H. M., Szczodrak, M., Thomson, J., Upchurch, L. M., Zhang, C., Zhang, D., & Zuidema, P. (2021). Measurements from the RV *Ronald H. Brown* and related platforms as part of the Atlantic Tradewind Ocean-Atmosphere Mesoscale Interaction Campaign (ATOMIC). *Earth System Science Data*, *13*(4), 1759–1790. https://doi.org/10.5194/ESSD-13-1759-2021

Rafaj, P., Amann, M., Siri, J., & Wuester, H. (2015). Changes in European greenhouse gas and air pollutant emissions 1960–2010: decomposition of determining factors. *Uncertainties in Greenhouse Gas Inventories*, 27–54. https://doi.org/10.1007/978-3-319-15901-0_3

Rickly, P. S., Guo, H., Campuzano-Jost, P., Jimenez, J. L., Wolfe, G. M., Bennett, R., Bourgeois, I., Crounse, J. D., Dibb, J. E., DiGangi, J. P., Diskin, G. S., Dollner, M., Gargulinski, E. M., Hall, S. R., Halliday, H. S., Hanisco, T. F., Hannun, R. A., Liao, J., Moore, R., Nault, B. A., Nowak, J. B., Peischl, J., Robinson, C. E., Ryerson, T., Sanchez, K. J., Schöberl, M., Soja, A. J., St Clair, J. M., Thornhill, K. L., Ullmann, K., Wennberg, P. O., Weinzierl, B., Wiggins, E. B., Winstead, E. L., & Rollins, A. W. (2022). Emission factors and evolution of $SO_2$ measured from biomass burning in wildfires and agricultural fires. *Atmos. Chem. Phys*, *22*, 15603–15620. https://doi.org/10.5194/acp-22-15603-2022

Roberts, G., Wooster, M. J., & Lagoudakis, E. (2009). Annual and diurnal African biomass burning temporal dynamics. *Biogeosciences*, *6*(5), 849–866. https://doi.org/10.5194/BG-6-849-2009

Rolph, G., Stein, A., & Stunder, B. (2017). Real-time Environmental Applications and Display sYstem: READY. *Environmental Modelling & Software*, *95*, 210–228.

Royer, H. M., Pöhlker, M. L., Krüger, O., Blades, E., Sealy, P., Lata, N. N., Cheng, Z., China, S., Ault, A. P., Quinn, P. K., Zuidema, P., Pöhlker, C., Pöschl, U., Andreae, M., & Gaston, C. J. (2023). African smoke particles act as cloud condensation nuclei in the wintertime tropical North Atlantic boundary layer over Barbados. *Atmospheric Chemistry and Physics*, *23*(2), 981–998. https://doi.org/10.5194/ACP-23-981-2023

Salvador, P., Almeida, S.M., Cardoso, J., Almeida-Silva, M., Nunes, T., Cerqueira, M., Alves, C., Reis, M.A., Chaves, P.C., Artínano, B., & Pio, C. (2015). Composition and origin of $PM_{10}$ in Cape Verde: Characterization of long-range transport episodes. *Atmospheric Environment*, *127*, 326-339.

Sarwar, G., Fahey, K. M., Napelenok, S. L., Roselle, S. J., & Mathur, R. (2011). Examining the impact of CMAQ model updates on aerosol sulfate predictions. In *The 10th Annual CMAS Models-3 User's Conference* (p. vol 775). Chapel Hill, NC.

Sarwar, Golam, Hogrefe, C., Henderson, B. H., Foley, K., Mathur, R., Murphy, B., & Ahmed, S. (2023). Characterizing variations in ambient $PM_{2.5}$ concentrations at the U.S. Embassy in Dhaka, Bangladesh using observations and the CMAQ modeling system. *Atmospheric Environment*, *296*, 119587. https://doi.org/10.1016/J.ATMOSENV.2023.119587

Saturno, J., Ditas, F., Penning De Vries, M., Holanda, B. A., Pöhlker, M. L., Carbone, S., Walter, D., Bobrowski, N., Brito, J., Chi, X., Gutmann, A., Hrabe De Angelis, I., Machado, L. A. T., Moran-Zuloaga, D., Rüdiger, J., Schneider, J., Schulz, C., Wang, Q., Wendisch, M., Artaxo, P., Wagner, T., Pöschl, U., Andreae, M. O., & Pöhlker, C. (2018). African volcanic emissions influencing atmospheric aerosol particles over the Amazon rain forest. *Atmospheric Chemistry and Physics*, *18*, 10391–10405. https://doi.org/10.5194/acp-2017-1152

Savoie, D. L., & Prospero, J. M.; (1980). Water-soluble potassium, calcium, and magnesium in the aerosols over the tropical North Atlantic. *Journal of Geophysical Research: Oceans*, *85*(C1), 385–392. https://doi.org/10.1029/JC085IC01P00385

Savoie, D. L., & Prospero, J. M. (1982). Particle size distribution of nitrate and sulfate in the marine atmosphere. *Geophysical Research Letters*, *9*(10), 1207–1210.

Savoie, D.L., Arimoto, R., Keene, W. C., Prospero, J. M., Duce, R. A., & Galloway, J. N. (2002). Marine biogenic and anthropogenic contributions to non-sea-salt sulfate in the marine boundary layer over the North Atlantic Ocean. *Journal of Geophysical Research-Atmospheres*, *107*(D18), 4356, doi:10.1029/2001JD000970.

Scheuvens, D., Schutz, L., Kandler, K., Ebert, M., & Weinbruch, S. (2013). Bulk composition of northern African dust and its source sediments - A compilation. *Earth-Science Reviews*, *116*, 170–194.

Schlosser, J. S., Braun, R. A., Bradley, T., Dadashazar, H., MacDonald, A. B., Aldhaif, A. A., Aghdam, M. A., Mardi, A. H., Xian, P., & Sorooshian, A. (2017). Analysis of aerosol composition data for western United States wildfires between 2005 and 2015: Dust emissions, chloride depletion, and most enhanced aerosol constituents. *Journal of Geophysical Research: Atmospheres*, *122*(16), 8951–8966. https://doi.org/10.1002/2017JD026547

Shah, V., Jaeglé, L., Thornton, J. A., Lopez-Hilfiker, F. D., Lee, B. H., Schroder, J. C., Campuzano-Jost, P., Jimenez, J. L., Guo, H., Sullivan, A. P., Weber, R. J., Green, J. R., Fiddler, M. N., Bililign, S., Campos, T. L., Stell, M., Weinheimer, A. J., Montzka, D. D., & Brown, S. S. (2018). Chemical feedbacks weaken the wintertime response of particulate sulfate and nitrate to emissions reductions over the eastern United States. *Proceedings of the National Academy of Sciences of the United States of America*, *115*(32), 8110–8115. https://doi.org/10.1073/PNAS.1803295115

Shikwambana, L., Mhangara, P., & Mbatha, N. (2020). Trend analysis and first time observations of sulphur dioxide and nitrogen dioxide in South Africa using TROPOMI/Sentinel-5 P data. *International Journal of Applied Earth Observation and Geoinformation*, *91*, 102130. https://doi.org/10.1016/J.JAG.2020.102130

Smith, S. J., Van Aardenne, J., Klimont, Z., Andres, R. J., Volke, A., & Delgado Arias, S. (2011). Anthropogenic sulfur dioxide emissions: 1850-2005. *Atmospheric Chemistry and Physics*, *11*(3), 1101–1116. https://doi.org/10.5194/ACP-11-1101-2011

Stein, A. F., Draxler, R. R., Rolph, G. D., Stunder, B. J. B., Cohen, M. D., & Ngan, F. (2015). NOAA's HYSPLIT Atmospheric Transport and Dispersion Modeling System. *Bulletin of the American Meteorological Society*, *96*(12), 2059–2077.

Taylor, S. R., & McLennan, S. M. ; (1985). *The continental crust: Its composition and evolution*. Oxford: Blackwell Scientific Publications.

Trapp, J. M., Millero, F. J., & Prospero, J. M. (2010). Trends in the solubility of iron in dust-dominated aerosols in the equatorial Atlantic trade winds: Importance of iron speciation and sources. *Geochemistry, Geophysics, Geosystems*, *11*(Q03014), doi:10.1029/2009GC002651.

Tsamalis, C., Chédin, A., Pelon, J., & Capelle, V. (2013). The seasonal vertical distribution of the Saharan Air Layer and its modulation by the wind. *Atmospheric Chemistry and Physics*, *13*(22), 11235–11257. https://doi.org/10.5194/ACP-13-11235-2013

Val, S., Liousse, C., Doumbia, E. H. T., Galy-Lacaux, C., Cachier, H., Marchand, N., Badel, A., Gardrat, E., Sylvestre, A., & Baeza-Squiban, A. (2013). Physico-chemical characterization of African urban aerosols (Bamako in Mali and Dakar in Senegal) and their toxic effects in human bronchial epithelial cells: Description of a worrying situation. *Particle and Fibre Toxicology*, *10*(1), 1–16. https://doi.org/10.1186/1743-8977-10-10/FIGURES/8

Vannucci, P. F., Foley, K., Murphy, B. N., Hogrefe, C., Cohen, R. C., & Pye, H. O. T. (2024). Temperature-dependent composition of summertime $PM_{2.5}$ in observations and model predictions across the Eastern U.S. *ACS Earth and Space Chemistry*, Submitted.

Vasilakos, P., Russell, A., Weber, R., & Nenes, A. (2018). Understanding nitrate formation in a world with less sulfate. *Atmospheric Chemistry and Physics*, *18*(17), 12765–12775. https://doi.org/10.5194/ACP-18-12765-2018

Wang, S., Maltrud, M., Elliott, S., Cameron-Smith, P., & Jonko, A. (2018). Influence of dimethyl sulfide on the carbon cycle and biological production. *Biogeochemistry*, *138*, 49–68. https://doi.org/10.1007/s10533-018-0430-5

Van der Werf, G. R., Randerson, J. T., Collatz, G. J., & Giglio, L. (2003). Carbon emissions from fires in tropical and subtropical ecosystems. *Global Change Biology*, *9*(4), 547–562. https://doi.org/10.1046/J.1365-2486.2003.00604.X

Wex, H., Dieckmann, K., Roberts, G. C., Conrath, T., Izaguirre, M. A., Hartmann, S., Herenz, P., Schafer, M., Ditas, F., Schmeissner, T., Henning, S., Wehner, B., Siebert, H., & Stratmann, F. (2016). Aerosol arriving on the Caribbean island of Barbados: physical properties and origin. *Atmospheric Chemistry and Physics*, *16*(22), 14107–14130.

Wiedinmyer, C., Akagi, S. K., Yokelson, R. J., Emmons, L. K., Al-Saadi, J. A., Orlando, J. J., & Soja, A. J. (2011). The Fire INventory from NCAR (FINN): a high resolution global model to estimate the emissions from open burning. *Geosci. Model Dev*, *4*, 625–641. https://doi.org/10.5194/gmd-4-625-2011

Wolter, K., & Timlin, M. S. (2011). El Niño/Southern Oscillation behaviour since 1871 as diagnosed in an extended multivariate ENSO index (MEI.ext). *International Journal of Climatology*, *31*(7), 1074–1087. https://doi.org/10.1002/JOC.2336

Yang, Y., Lou, S., Wang, H., Wang, P., & Liao, H. (2020). Trends and source apportionment of aerosols in Europe during 1980-2018. *Atmospheric Chemistry and Physics*, *20*(4), 2579–2590. https://doi.org/10.5194/ACP-20-2579-2020

Zhang, T., Hoell, A., Perlwitz, J., Eischeid, J., Murray, D., Hoerling, M., & Hamill, T. M. (2019). Towards probabilistic multivariate ENSO monitoring. *Geophysical Research Letters*, *46*(17–18), 10532–10540. https://doi.org/10.1029/2019GL083946

Zhao, B., Jiang, J. H., Gu, Y., Diner, D., Worden, J., Liou, K. N., Su, H., Xing, J., Garay, M., & Huang, L. (2017). Decadal-scale trends in regional aerosol particle properties and their linkage to emission changes. *Environmental Research Letters*, *12*(5), 054021. https://doi.org/10.1088/1748-9326/AA6CB2

Zhao, J., Zhang, Y., Bie, S., Bilsback, K. R., Pierce, J. R., & Chen, Y. (2024). Changes in global DMS production driven by increased $CO_2$ levels and its impact on radiative forcing. *Npj Climate and Atmospheric Science 2024 7:1*, *7*(1), 1–8. https://doi.org/10.1038/s41612-024-00563-y

Zubkova, M., Boschetti, L., Abatzoglou, J. T., & Giglio, L. (2019). Changes in fire activity in Africa from 2002 to 2016 and their potential drivers. *Geophysical Research Letters*, *46*, 7643–7653. https://doi.org/10.1029/2019GL083469

Zuidema, P., Redemann, J., Haywood, J., Wood, R., Piketh, S., Hipondoka, M., & Formenti, P. (2016). Smoke and clouds above the Southeast Atlantic: Upcoming field campaigns probe absorbing aerosol's impact on climate. *Bulletin of the American Meteorological Society*, *97*(7), 1131–1135. https://doi.org/10.1175/BAMS-D-15-00082.1

Zuidema, P., Sedlacek, A. J., Flynn, C., Springston, S., Delgadillo, R., Zhang, J., Aiken, A. C., Koontz, A., & Muradyan, P. (2018). The Ascension Island boundary layer in the remote Southeast Atlantic is often smoky. *Geophysical Research Letters*, *45*(9), 4456–4465. https://doi.org/10.1002/2017GL076926

Zuidema, P., Alvarez, C., Kramer, S. J., Custals, L., Izaguirre, M., Sealy, P., Prospero, J. M., & Blades, E. (2019). Is summer African dust arriving earlier to Barbados? The updated long-term in situ dust mass concentration time series from Ragged Point, Barbados, and Miami, Florida. *Bulletin of the American Meteorological Society*, *100*(10), 1981–1986. https://doi.org/10.1175/BAMS-D-18-0083.1